AN EXPERIMENTAL INVESTIGATION OF THE DRAG ON A CIRCULAR CYLINDER AND CURVED SHELL IN TRANSONIC FLOW

Steve Borah

Air Force Institute of Technology
Wright-Patterson Air Force Base, Ohio

December 1975

DISCLAIMER NOTICE

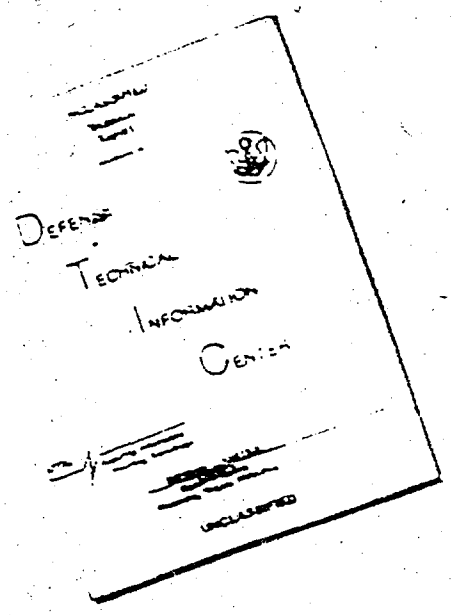

THIS DOCUMENT IS BEST QUALITY AVAILABLE. THE COPY FURNISHED TO DTIC CONTAINED A SIGNIFICANT NUMBER OF PAGES WHICH DO NOT REPRODUCE LEGIBLY.

AN EXPERIMENTAL INVESTIGATION OF THE DRAG ON A CIRCULAR CYLINDER AND CURVED SHELL IN TRANSONIC FLOW

THESIS

GAE/AE/75D-8

Steve Borah
Capt USAF

SECURITY CLASSIFICATION OF THIS PAGE (When Data Entered)

REPORT DOCUMENTATION PAGE		READ INSTRUCTIONS BEFORE COMPLETING FORM
1. REPORT NUMBER GAE/AE/75D-8	2. GOVT ACCESSION NO.	3. RECIPIENT'S CATALOG NUMBER
4. TITLE (and Subtitle) AN EXPERIMENTAL INVESTIGATION OF THE DRAG ON A CIRCULAR CYLINDER AND CURVED SHELL IN TRANSONIC FLOW		5. TYPE OF REPORT & PERIOD COVERED AFIT THESIS 6. PERFORMING ORG. REPORT NUMBER
7. AUTHOR(s) Steve Borah CAPT USAF		8. CONTRACT OR GRANT NUMBER(s)
9. PERFORMING ORGANIZATION NAME AND ADDRESS Air Force Insititute of Technology Wright-Patterson AFB, Ohio 45433		10. PROGRAM ELEMENT, PROJECT, TASK AREA & WORK UNIT NUMBERS
11. CONTROLLING OFFICE NAME AND ADDRESS		12. REPORT DATE December, 1975 13. NUMBER OF PAGES 96
14. MONITORING AGENCY NAME & ADDRESS(if different from Controlling Office) Air Force Flight Dynamics Laboratory Wright-Patterson AFB, Ohio 45433		15. SECURITY CLASS. (of this report) Unclassified 15a. DECLASSIFICATION/DOWNGRADING SCHEDULE

16. DISTRIBUTION STATEMENT (of this Report)

Approved for public release; distribution unlimited.

17. DISTRIBUTION STATEMENT (of the abstract entered in Block 20, if different from Report)

18. SUPPLEMENTARY NOTES

Approved for public release: IAW AFR/190-17

JERRY C. HIX, Capt, USAF
Director of Information

19. KEY WORDS (Continue on reverse side if necessary and identify by block number)

Drag
Transonic
Turret
Cavity Flow

20. ABSTRACT (Continue on reverse side if necessary and identify by block number)

This study was one in a series by the Air Force Flight Dynamics Laboratory in large turret aerodynamic research. The objective of the study was the reduction of transonic drag of a particular turret configuration by the addition of area rule fairings.

Wind tunnel models were tested at transonic Mach numbers from 0.6 to 0.9. An internally mounted force balance and unsteady pressure transducers were used to measure the forces

DD FORM 1 JAN 73 1473 EDITION OF 1 NOV 65 IS OBSOLETE Unclassified

1a SECURITY CLASSIFICATION OF THIS PAGE (When Data Entered)

- and pressure variations on the model. Fairings were placed beside and aft of the turret in an effort to reduce the transonic turret drag.

The least frag configuration was a single fairing mounted behind the turret. This design had as much as a 55% drag reduction from the bare turret. This mddel also created the smallest pressure fluctuations in a circular cavity in the side of the turret. Analysis of the drag data, oil flow patterns, and the normal area distributions of the different models indicated that simple far field area rule was not sufficient to determine the least drag configuration. Empirical analysis appears to be the only reliable method for studying drag reductions of large protuberances in transonic flow.

GAE/AE/75D-8

AN EXPERIMENTAL INVESTIGATION OF THE DRAG ON A CIRCULAR CYLINDER AND CURVED SHELL IN TRANSONIC FLOW

THESIS

Presented to the Faculty of the School of Engineering
of the Air Force Institute of Technology
Air University
in Partial Fulfillment of the
Requirements for the Degree of
Master of Science

by

Steve B. Borah, B.S.
Captain USAF

Graduate Aerospace and Mechanical Engineering
December 1975

ic

Preface

The drag reduction of an aircraft is an even more important endeavor today because of energy considerations. This experimental investigation was a continuation of the work started by Dr. James Van Kuren into the area of drag reduction for large excresances on transport aircraft. The results of this work confirm Dr. Van Kuren's findings and suggest that a simple method such as area rule distribution does not predict the optimum design. The optimum design for a given protuberance will have to be empirically determined for transonic flow. Hopefully, the results of this study will provide both a data base and a guide for future designers.

I would like to thank Dr. James Van Kuren of the Flight Dynamics Laboratory and Major Roger Crawford of the Air Force Institute of Technology, who together advised my efforts. Mr. Ron Walterick of the Flight Dynamics Laboratory deserves special notice for his assistance and counsel during all phases of this test. Additionally, I would like to thank Mr. Wolfe and his staff at the AFIT machine shop for their professionalism in preparing my model.

Lastly, I would like to acknowledge the love and undying devotion of my wife, who through this difficult and trying period in our lives, showed an extreme amount of patience and understanding.

Steve B. Borah

Table of Contents

List of Figures

List of Figures

List of Tables

List of Symbols

C_D	Drag Coefficient
CONF	Configuration or Model
C_P	Coefficient of Pressure
db	Decibels
DFA	Dorsal Fin A
DFB	Dorsal Fin B
Irig B	Time Code Language
LSF	Large Side Fairing
M	Mach Number
P_{rms}	Root Mean Square of Unsteady Pressure
PSD	Power Spectral Density
q	Dynamic Pressure
RMS	Root Mean Square
SSF	Small Side Fairing
S_t	Reference Area, Frontal Area of Turret, 0.047 ft^2
$\Delta 1$	Turret Azimuth Angle
$\Delta 2$	Turret Elevation Angle

Abstract

This study was one in a series by the Air Force Flight Dynamics Laboratory in large turret aerodynamic research. The objective of the study was the reduction of transonic drag of a particular turret configuration by the addition of area rule fairings.

Wind tunnel models were tested at transonic Mach numbers from 0.6 to 0.9. An internally mounted force balance and unsteady pressure transducers were used to measure the forces and pressure variations on the model. Fairings were placed beside and aft of the turret in an effort to reduce the transonic turret drag.

The least drag configuration was a single fairing mounted behind the turret. This design had as much as a 55% drag reduction from the bare turret. This model also created the smallest pressure fluctuations in a circular cavity in the side of the turret. Analysis of the drag data, oil flow patterns, and the normal area distributions of the different models indicated that simple far field area rule was not sufficient to determine the least drag configuration. Empirical analysis appears to be the only reliable method for studying drag reductions of large protuberances in transonic flow.

AN EXPERIMENTAL INVESTIGATION OF THE DRAG ON A CIRCULAR CYLINDER AND CURVED SHELL IN TRANSONIC FLOW

I. Introduction

Background

The transonic flow field is very difficult to analyze theoretically because the governing equations are basically nonlinear. The existence of both subsonic and supersonic flow on a body in this region yields a complicated flow pattern. This mixed flow field plus the effects of shock wave and boundary layer interaction make transonic flow a region where it is almost impossible to determine by theoretical methods what the drag will be on any arbitrary body shape.

An unexplored region of transonic flow is the drag of large protuberances on a body. Many of today's military aircraft have protuberances, such as cylinders, on their bodies and wings. A cylinder with its longitudinal axis perpendicular to the freestream velocity creates a large amount of drag because of its bluntness and flow separation from its aft surface. Such a cylinder mounted to the fuselage of a large transport aircraft, depending on its relative size, could create as much as 15% of the total drag of the airplane.

Problem

The object of this test is to reduce the transonic drag of a turret mounted on an aircraft fuselage. The shape of the turret for this test is a right circular cylinder with a hemispherical cap on the top and a circular cavity in the side, Fig 1. This turret will be mounted perpendicular to a curved fuselage surface.

Gaudet and Winter conducted an investigation into the increment of drag due to various excrecenses at varying Mach numbers and Reynolds numbers (Ref 1). Unfortunately, all of their testing was conducted at either subsonic or supersonic velocities because of the capability of their wind tunnel. No transonic tests were conducted. The results they obtained for subsonic drag on a turret indicate that the drag can be approximated by two components. One component is the drag on the turret in the boundary layer and the other component is the drag in the freestream. Transonic flow does not allow the superposition of drag increments because of the complex boundary layer and shock wave interactions. The results of Gaudet and Winter for supersonic flow show that the value of the drag increased with increases in Reynolds number (Ref 1:13).

Transonic tests of the particular protuberance, a right circular cylinder with a hemispherical end mounted perpendicular to a curved shell, have been conducted. Dr. Van Kuren has investigated the reduction of drag on the particular body combination by the addition of splitter plates fore and aft of the cylinder and a

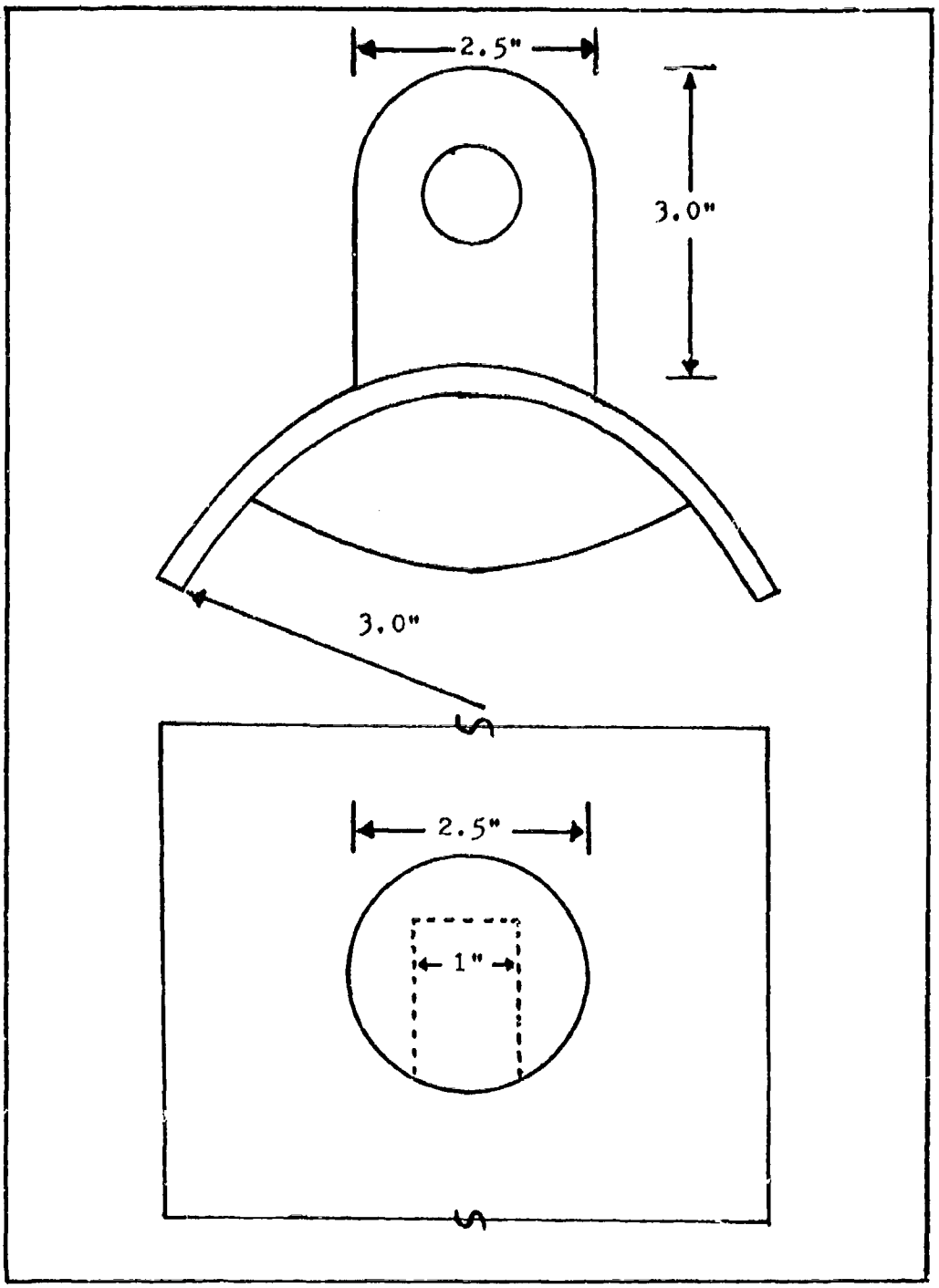

Fig. 1. Front and Top View of Turret

non-interference fairing on the curved shell (Ref 2:2). This configuration showed a decrease in the transonic drag but further testing of other configurations was indicated. Other configurations, mainly fairings aft of the cylinder were tested in an effort to reduce the transonic drag (Ref 3). Because of aft fairing structural limitations and the lack of instrumentation, these tests did not analyze all the possible fairing configurations. The configurations that were tested reduced the drag on a bare turret be 50% (Ref 3:19).

Scope

This experimental investigation was an extension of the tests conducted by Van Kuren. It was desired to confirm the previous test results and determine whether other designs may create less drag for the basic body combination of curved shell and circular cylinder, while maintaining the same flow dynamics in the turret cavity.

In an effort to determine minimum drag shapes, the basic model and various fairing shapes were tested at transonic velocities in the Tri-sonic Gasdynamic Facility of the Air Force Flight Dynamics Laboratory, Wright-Patterson Air Force Base, Ohio.

The concept of transonic area ruling, having a streamlined cross-sectional area distribution, was used as a guideline in determining the possible fairing shapes to be tested. Generally, the shape of a compound body should be

such that a smooth cross-sectional area distribution is created. The non-interference fairings and aft fairings plus fairings mounted beside the turret were tested individually and in combinations to achieve this result. Thus, it was possible to determine the incremental effects of each component and the interference effects of one upon the other.

During the testing, six component force data of the model, and steady and unsteady static pressures on the model surface were measured. The Mach number range for testing was from 0.6 to 0.9 at a constant Reynolds number. The only other test variables were the turret azimuth angle $\Delta 1$ and elevation angle $\Delta 2$.

II. Description of Apparatus

Model

Two models were used during the wind tunnel tests. Model A was an aluminum shell 29" long with a radius of curvature of three inches. Model B was an aluminum shell 29" long with a radius of curvature of three inches, and had an epoxy noninterference fairing mounted on top of the shell fore and aft of the turret location. A curved shell was used instead of a blunt or rounded cylinder in order to simulate the flow and boundary layer along the fuselage of a large transport aircraft. A blunt body of revolution would have created too large of a boundary layer region.

The turret was a right circular cylinder 2.5" in diameter and 3" high with a hemispherical top and a 1" circular cavity in the forward side. The models were internally equiped with an electric motor to turn the turret in azimuth and a rotary potentiometer to measure the azimuth position. The turret could be manually rotated in elevation. The turret was mounted 12" from the leading edge on either model A or B. When mounted in the test section, the cavity in the turret was on the approximate centerline of the wind tunnel, Fig 2.

Table I contains a brief description of all the configurations. Drawings for each configuration can be found in Appendix A.

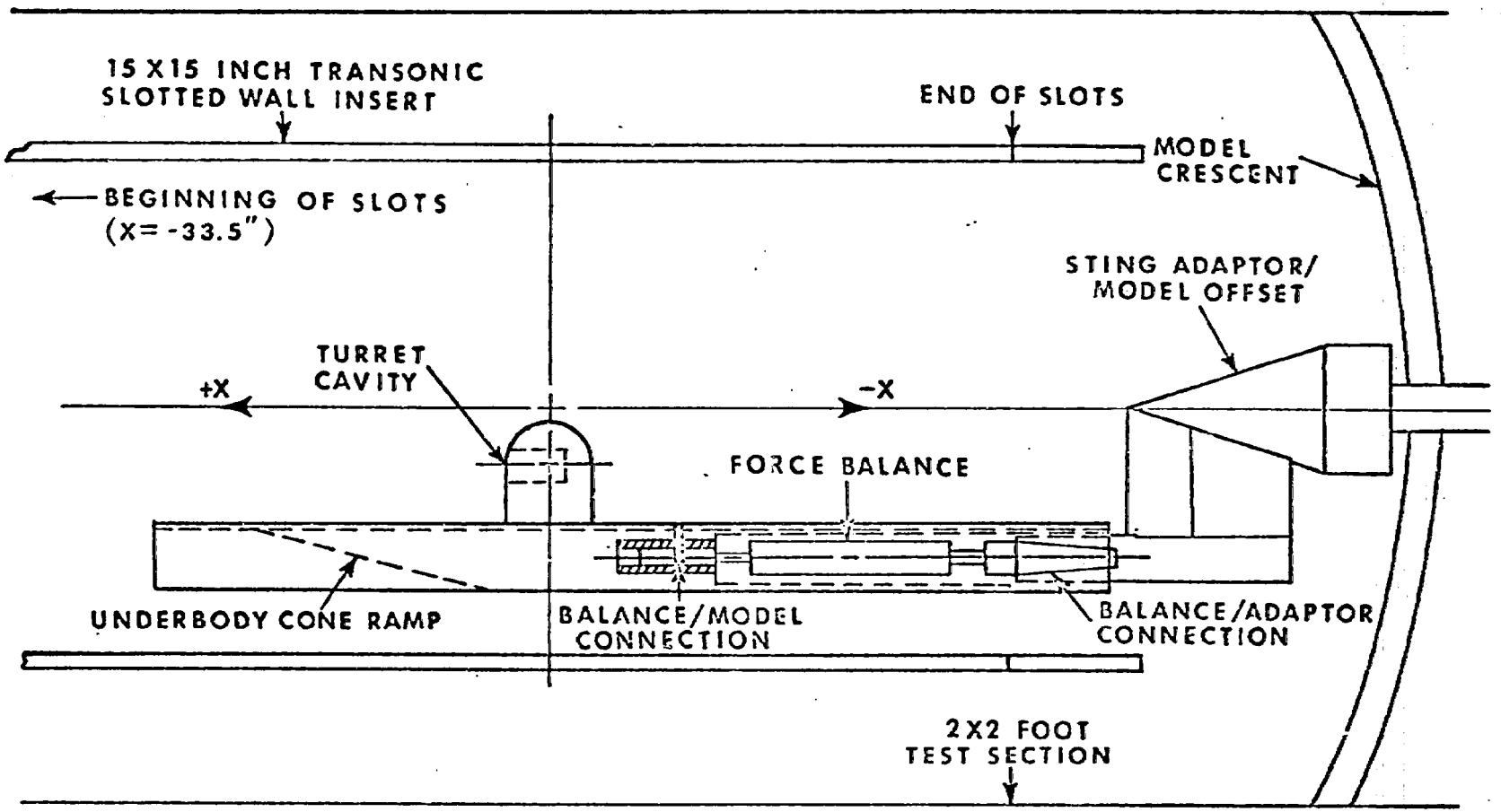

FIGURE 2 TEST ARRANGEMENT

Table I List of Models

Model	Description	
1	Plain Shell	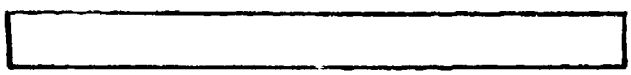
2	Plain Shell & Turret	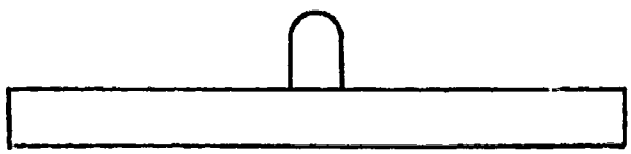
3	Model 2 & Ramps & Dorsal Fin A & Large Side Fairings	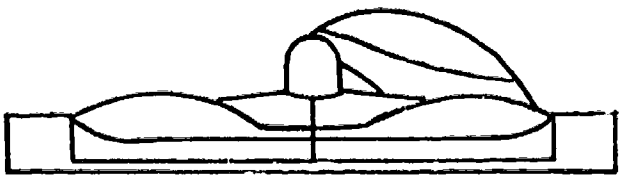
4	Model 2 & Ramps & Dorsal Fin A & Small Side Fairings	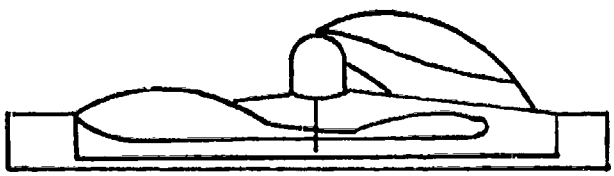
5	Model 2 & Ramps & Dorsal Fin A	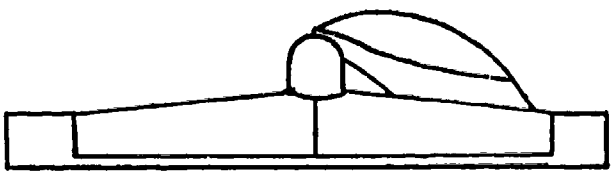
6	Model 2 & Ramps & Dorsal Fin B	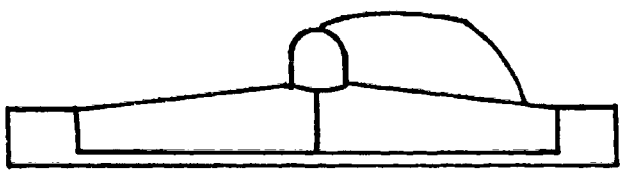
7	Model 2 & Ramps & Dorsal Fin B & Small Side Fairings	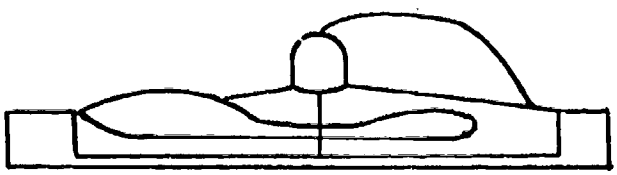

Fairings

The two basic configurations could be changed by the addition of various fairings. The purpose of the fairings was to change the local area distribution of the model to improve the local streamline flow. Because the turret was so blunt and flow separation occurred from the aft surface, Van Kuren experimently determined the shape of aft fairings to improve the streamline flow (Ref 3). He also recommended that fairings beside the turret be tested to see if they improved the streamline flow and reduced the drag. Two of the fairings tested were dorsal fins mounted behind the turret. Dorsal fin A (DFA) was thinner and had a smaller cross-sectional area distribution than dorsal fin B (DFB). Dorsal fin B was found to create the least drag.

Two sets of fairings tested could be mounted along the shell beside the turret. The large side fairings (LSF) were symmetrical on each side fore and aft of the turret lateral centerline and the left side was symmetrical with the right side. The small side fairings (SSF) were symmetrical from side to side, but the aft sections were smaller in cross-sectional area than the fairings forward of the turret. The area distribution that resulted from the use of aft and side fairings is given in Figs 3 and 4.

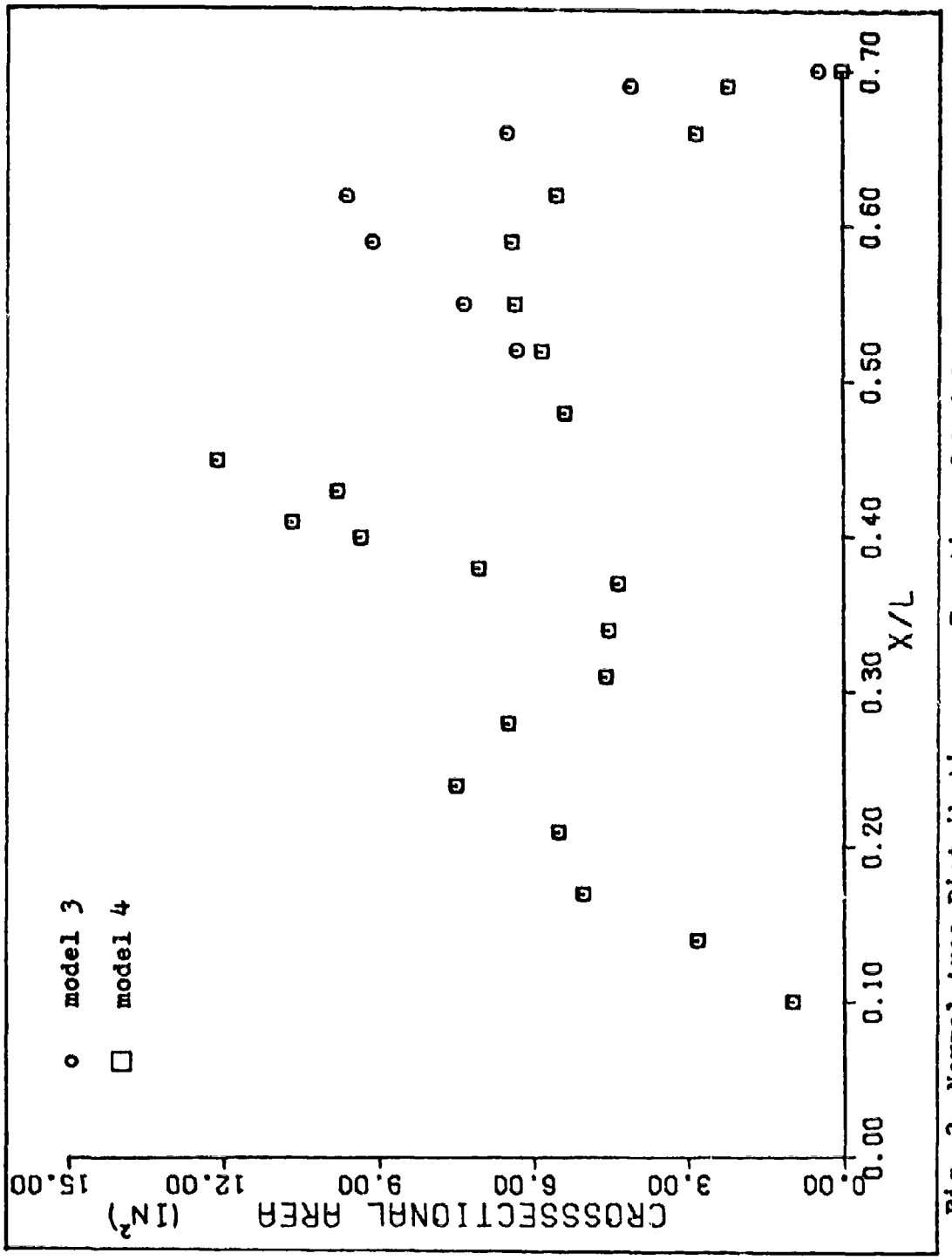

Fig. 3. Normal Area Distribution as a Function of Model Length

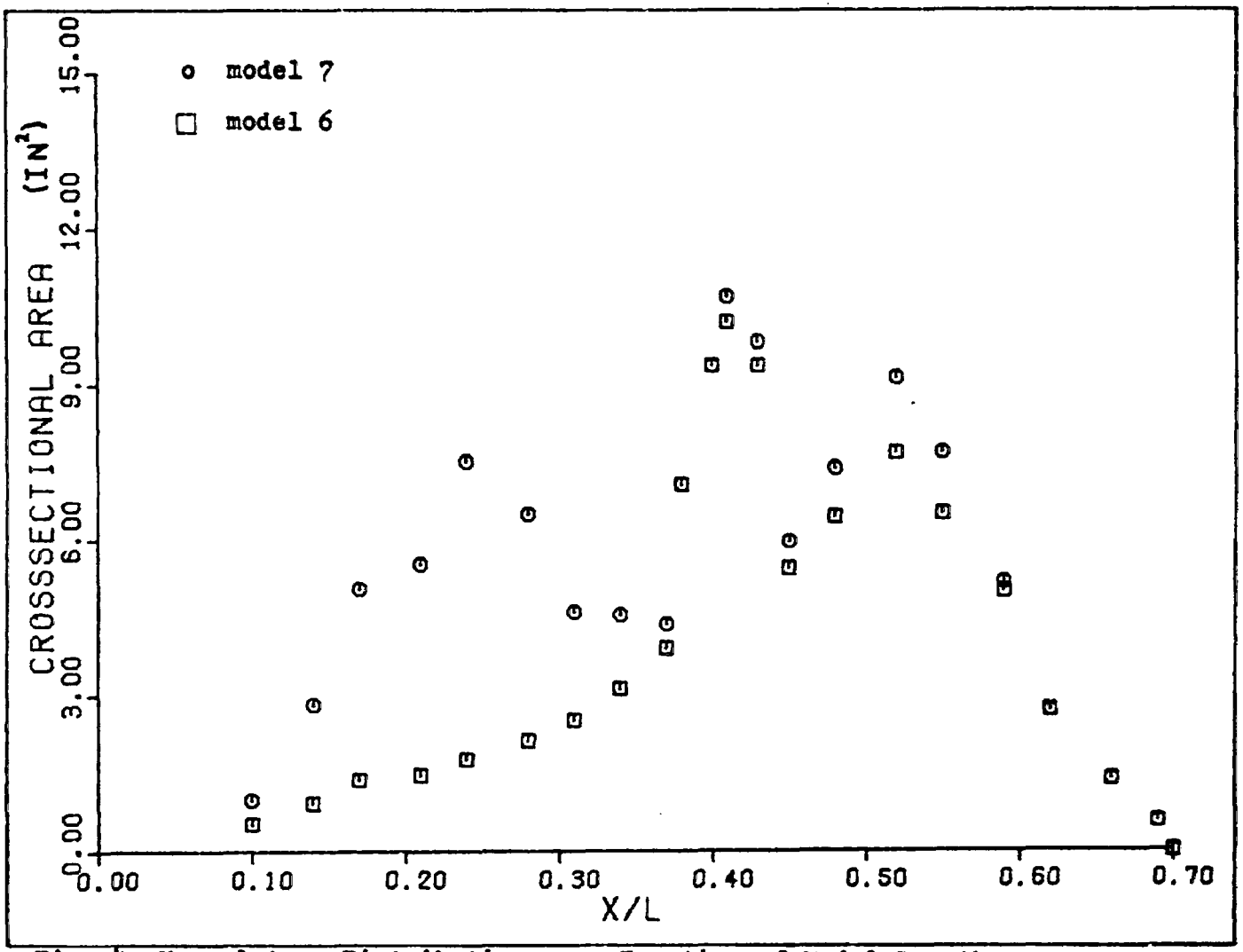

Fig. 4. Normal Area Distribution as a Function of Model Length

A curved circular plate could be mounted in place of the turret. The plate was tested with model A to determine the baseline value of drag due to the shell, ventral fairing and the sting mounting. Illustrations of all configurations can be found in Appendix A.

Instrumentation

Both models A and B were mounted on the six component force balance for testing. This was the only instrumentation provided on model A. Model B was instrumented with 16 static pressure orifices along the model centerline and six locations for unsteady pressure transducers, Fig 5. This provided a pressure distribution on the model as a function of position and time. The turret was instrumented with one unsteady pressure transducer in the back wall of the cavity, Fig 5. This transducer was used to measure the pressure fluctuation of the flow in the cavity.

Wind Tunnel

The USAF Flight Dynamics Laboratory Tri-sonic Gasdynamic Facility was used in this investigation. A 15" by 15" transonic test section was used with slotted walls of 10% porosity, Fig 2. The slotted transonic tunnel allowed all of the configurations to be tested in a range of Mach numbers from 0.6 to 0.9. This was important because of the large size of the model and the fact that the model blockage factor was as high as 9%.

+ = STATIC PRESSURE ORIFICES

⊕ = DYNAMIC PRESSURE TRANSDUCERS

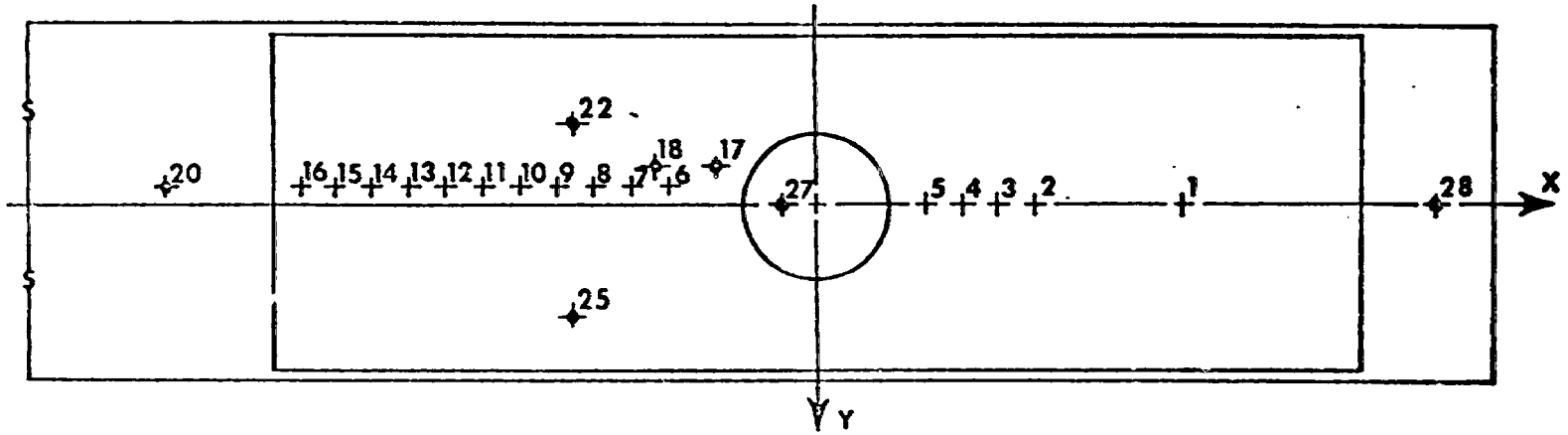

DYNAMIC PRESSURE TRANSDUCERS

KULITE ※	X(in)	Y(in)
17	1.65	-.616
18	2.75	-.616
20	11.0	-.255
22	4.125	-1.334
25	4.125	1.927
27	TURRET *	
28	10.625	0.0

STATIC PRESSURE ORIFICES

ORIFICE ※	X(in)	Y(in)	ORIFICE ※	X(in)	Y(in)
1	6.25	0.0	9	-4.38	.25
2	3.75	0.0	10	-5.0	.25
3	3.125	0.0	11	-5.63	.25
4	2.5	0.0	12	-6.25	.25
5	1.875	0.0	13	-6.88	.25
6	-2.5	.25	14	-7.5	.25
7	-3.13	.25	15	-8.13	.25
8	-3.75	-25	16	-8.75	.25

* Number 27 is mounted in the back wall of the cavity

FIGURE 5 MODEL INSTRUMENTATION LOCATIONS ON CONFIGURATION 02

The slotted walls of 10% porosity reduced the transonic drag increase because of model blockage. The test section was equipped with the capability to measure dynamic force and pressure data along with steady pressure information. This greatly reduced the amount of test time required. Complete details of this facility can be found in reference 4.

Data Acquisition System

The following is a brief description of the components that were part of the data acquisition system. A schematic of the way in which this equipment was connected is given in Fig 6.

Computer. The instrumentation on the model interfaced with a Hewlett-Packard multiplexer and digital computer. The computer was used to compute the coefficients of force and pressure from the transducer voltages. These computations were made on line as each test point was taken and then stored on a disc memory for later analysis.

Force Balance. An internal strain gauge balance, Air Force Flight Dynamics Laboratory model 6SW-60-20-30, was used to determine the forces on the model during the test. The model was designed so the balance was completely enclosed by the ventral fairing. By mounting the model to the balance and the balance to the sting in the test section, the six force components, lift, drag, side force (yaw), pitching moment, yawing moment, and rolling moment could be measured directly.

Because pressure data was measured at the same time force measurements were being taken, it was necessary to bridge the balance with several wires and pressure tubes. Icardi bridged a force balance in a similiar manner during his testing and he experienced approximately a 0.1% error in the data (Ref 5:12).

Pressure Transducers. Kulite model XCQL-14-093-25 high frequency response, variable reference pressure transducers were installed in the model to measure the unsteady pressures. These instruments have temperature compensating units and are responsive to input frequencies of up to 20 KHz. The unsteady pressure survey from the Kulite transducers provided a pressure map as a function of time on the model's surface. The Kulite mounted in the turret cavity provided a pressure analysis as a function of time and turret angle.

Fourier Analyzer. A Hewlett-Packard model 3721A Fourier Analyzer was used to generate a power spectral density PSD graph from the unsteady pressure data. The input bandwidth for this instrument was 10 Hz. The analyzer sampled the unsteady pressure data 1000 times and then used a standard Fourier analysis technique to obtain the PSD. The computer was programed to do a search routine of the PSD to determine the maximum power values and their corresponding frequencies. A minimum change of 5 decibels was required for a peak to qualify as a maximum. The maximum power values

in decibels and their corresponding frequencies were then stored on the computer memory along with the static data.

Tape Recorder. Unsteady pressure data was recorded by an Ampex model CP100, 14 channel, FM, tape recorder. This recorder had a maximum frequency response of 80 KHz and a maximum input voltage limit of 1.4 volts per channel. Input signals were monitored on an oscilloscope to insure they were within frequency and voltage limits. Irig B was coded on one channel so the data tape could be used at a later time for data reduction. This reduced the amount of time required for each test run.

RMS Meter. The output signals of the pressure transducers went through a Hewlett-Packard model 3400A root mean square voltmeter. This instrument had a two second integration time to obtain an RMS voltage. By multiplying this voltage by the transducer constant, the root mean square of the unsteady pressure P_{rms} was obtained. P_{rms} was the unsteady pressure input recorded by the FM tape recorder.

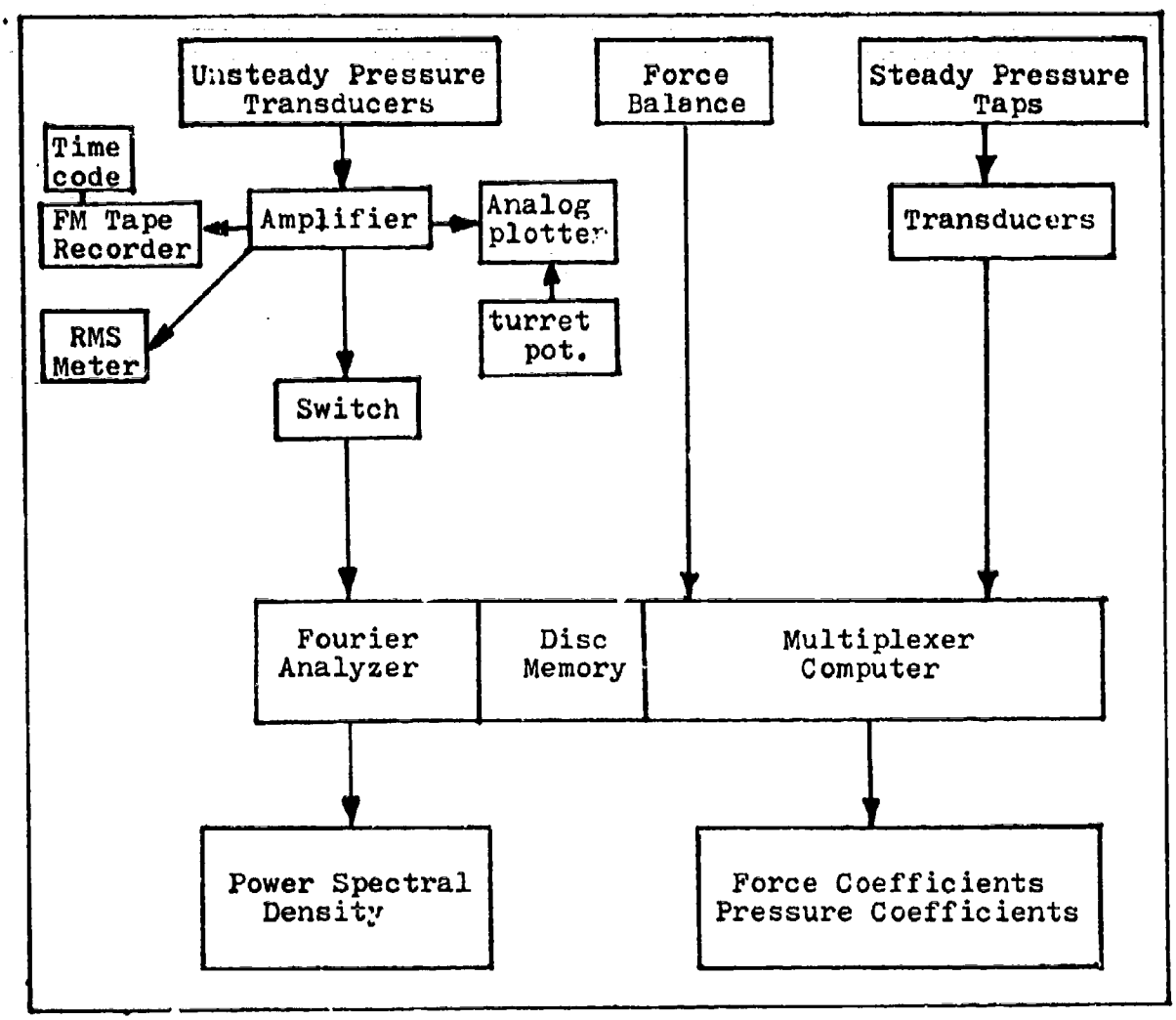

Fig. 6. Schematic of Data Acquisition System

III. Experimental Procedures

The test program can be divided into three phases, calibration, model testing, and flow visualization. Figure 6 shows a schematic of the test instrumentation.

Calibration

The force balance for the test was connected to the computer and calibrated by comparing known loads on the balance with the computer printout. The balance error was less than 1% of full scale reading during calibration and remained that during check loadings after each model change. Complete details of the balance calibration and the calculation of the balance coefficients is available from the Flight Mechanics Division, Air Force Flight Dynamics Laboratory.

The azimuth angle $\Delta 1$ of the turret was calibrated by using a rotary potentiometer mounted in the model. Zero angle for the cavity opening was set with the cavity opening normal to the freestream. Ninety degrees of angle was set with the turret rotated clockwise until the cavity opening was parallel to the freestream direction. The potentiometer readings were linear for turret rotation so they were used directly as an input for plotting P_{rms} versus $\Delta 1$ on the analog plotter.

The initial runs of the wind tunnel were used to determine the optimum settings of the diffuser flaps for

the transonic section. The setting of the diffuser flaps was varied until the static pressure measured on the model matched that of the freestream pressure. Goethert has reported that for subsonic Mach numbers in a slotted test section a ratio of test section static pressure P_d to plenum chamber static pressure P_c of 0.975 gave a correct indication of the proper combination of mass removal and tunnel compressor boost (Ref 6:331). With this proper combination, there were no variations in pressure along the test section that could produce erroneous drag readings. An optimum setting of full open for the diffuser flaps was used throughout the test.

Model Testing

Pope's recommended procedures for data taking were used for this test (Ref 7:188). Balance readings were taken before every test run to ensure there were no forces on the model. For each Mach number, the deflection of the balance wax compensated for by pitching the model in the opposite direction a corresponding amount. This procedure was necessary because the force balance used was very flexible. The balance deflected 7 min for every 3 lbs of normal force. This resulted in total deflections of as much as 1° during the test. Matching the deflection angle and pitching angle was necessary to standardize the test conditions of zero angle of attack for the model.

After the Mach number and pitch angle were established, the force and steady pressure data were read by the computer. Then, the seven RMS meters were recorded for one minute on the FM tape as the Fourier Analyzer was used to scan the PSD's of all the unsteady pressure transducers. The PSD's of selected transducers were stored in the computer memory.

Next, the turret azimuth angle $\Delta 1$ was varied from 0^{o} to 120^{o} as P_{rms} from the transducer in the turret cavity was plotted versus turret angle. Then, the turret was positioned at 90^{o} of azimuth and all the force, steady and unsteady pressure data were recorded as described for 0^{o} above.

This constituted one test point. The Mach number was changed and all the data was recorded for the next test point. Each configuration was tested at Mach numbers between 0.6 and 0.9 and turret angles of 0^{o} and 90^{o}, except model 1 which did not have a turret.

To determine the repeatability of the data, random test points were repeated during a test run and data readings were taken at the completion of each run. Some configurations were repeated at different times during the test to further validate the data, Fig 7 is a typical example.

The test was conducted at a constant unit Reynolds number of 2×10^{6}. Several configurations were tested at a Reynolds number of 3×10^{6} to determine any differences caused by viscous effects.

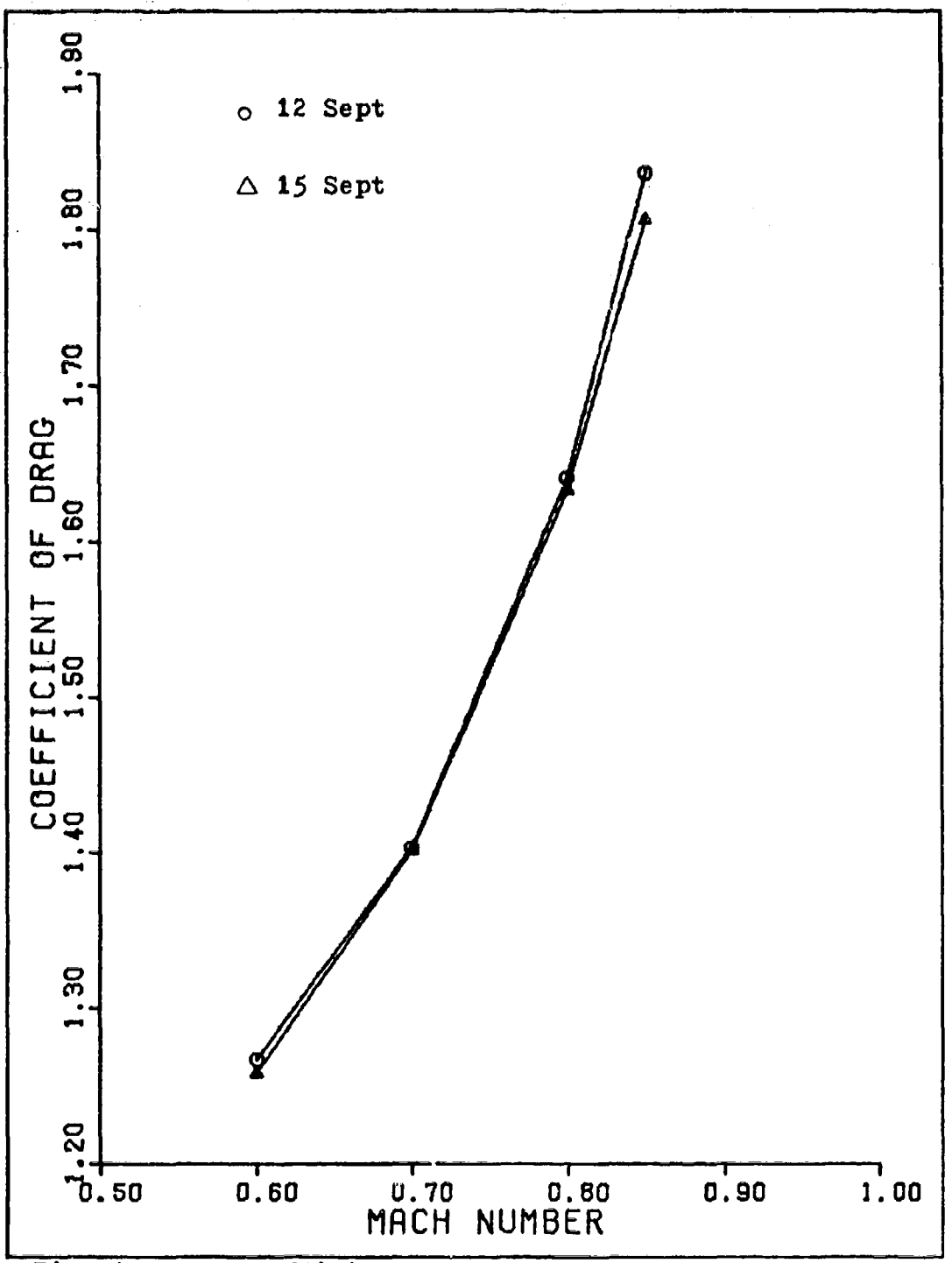

Fig. 7. Drag Coefficients for Model 2 from Two Different Days of testing

Because the force balance was bridged by wires and tubes during the test, several runs were made to analyze their effect on the data. The difference between test points with and without the balance bridged was approximatly 3% of the measured values, which correspondes to Icardi's 1% variation of full scale.

After the least drag configuration was determined, it was tested at elevation angles of the cavity of 15° and 30°. This was to record the pressure fluctuations in the cavity and determine whether there was any resonance present.

Oil Flow

Standard oil flow visualization techniques were used for this part of the test. A mixture of STP oil treatment, oleic acid, and titanium dioxide was painted on the model before each test run. For each Mach number, an oil streak pattern was formed by the boundary air flow around the model. These patterns were then sketched on drawings of the models.

The oil flow patterns indicated the location of stagnation streamlines and flow separation points. By proper application of the oil mixture, patterns of local streamline flow were formed. Knowing the streamline flow and areas of flow stagnation and separation was useful in determining the shape of fairings to reduce the turret drag.

IV. Results

Drag

The drag values presented in this section are defined to be the forces on the model in the axial direction as measured by the internally mounted force balance. The drag coefficients presented are the drag values divided by the dynamic pressure q and the reference area S_t, which was the frontal area of the turret, 0.047 ft^2.

Figure 7 shows an example of the repeatability of the drag data which was obtained on two different days for the same configuration. The largest error was approximately 2% of the first run value. Figure 8 shows the effect of the hysteresis in the force balance on the data for one day's test run. The repeated points are indistinguishable from the first test points. Figure 9 is a graph of the drag for a configuration with and without the force balance bridged. Based on the coefficient of drag with the balance bridged, the largest difference was 2%. From these three graphs, it is apparent that the data was accurate and repeatable. Based on these graphs and others, the results from this test could be reproduced within 3% of the optimum drag coefficient.

In an effort to determine the contribution of each body component to the total drag, incremental drag coefficients were calculated. The drag values for model 1 were substracted from those of the other models to find the incremental changes. Figure 10 shows a graph of the drag coefficients for models 1 and 2.

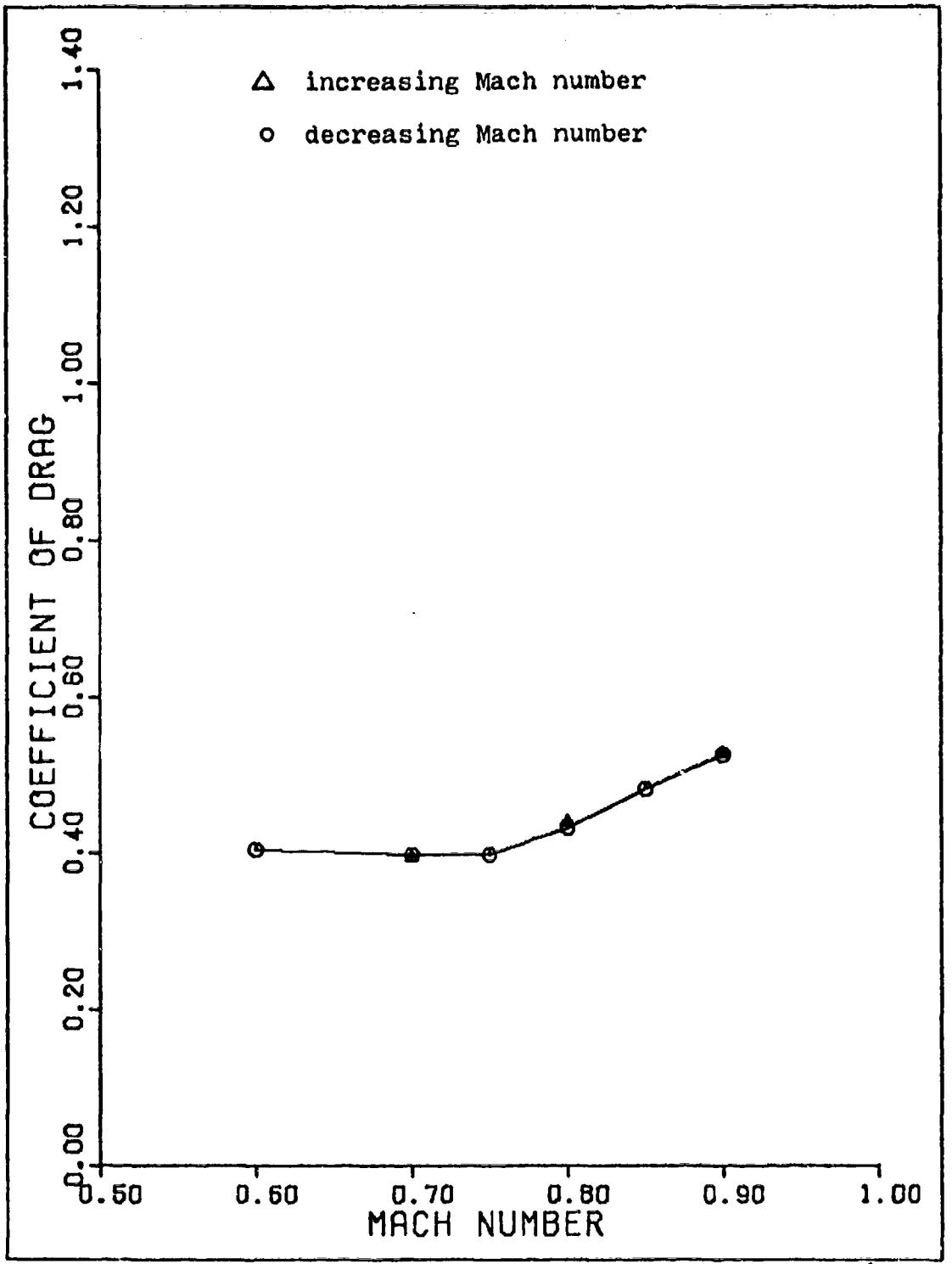

Fig. 8. Incremental C_D's for One Test Run of Model 6

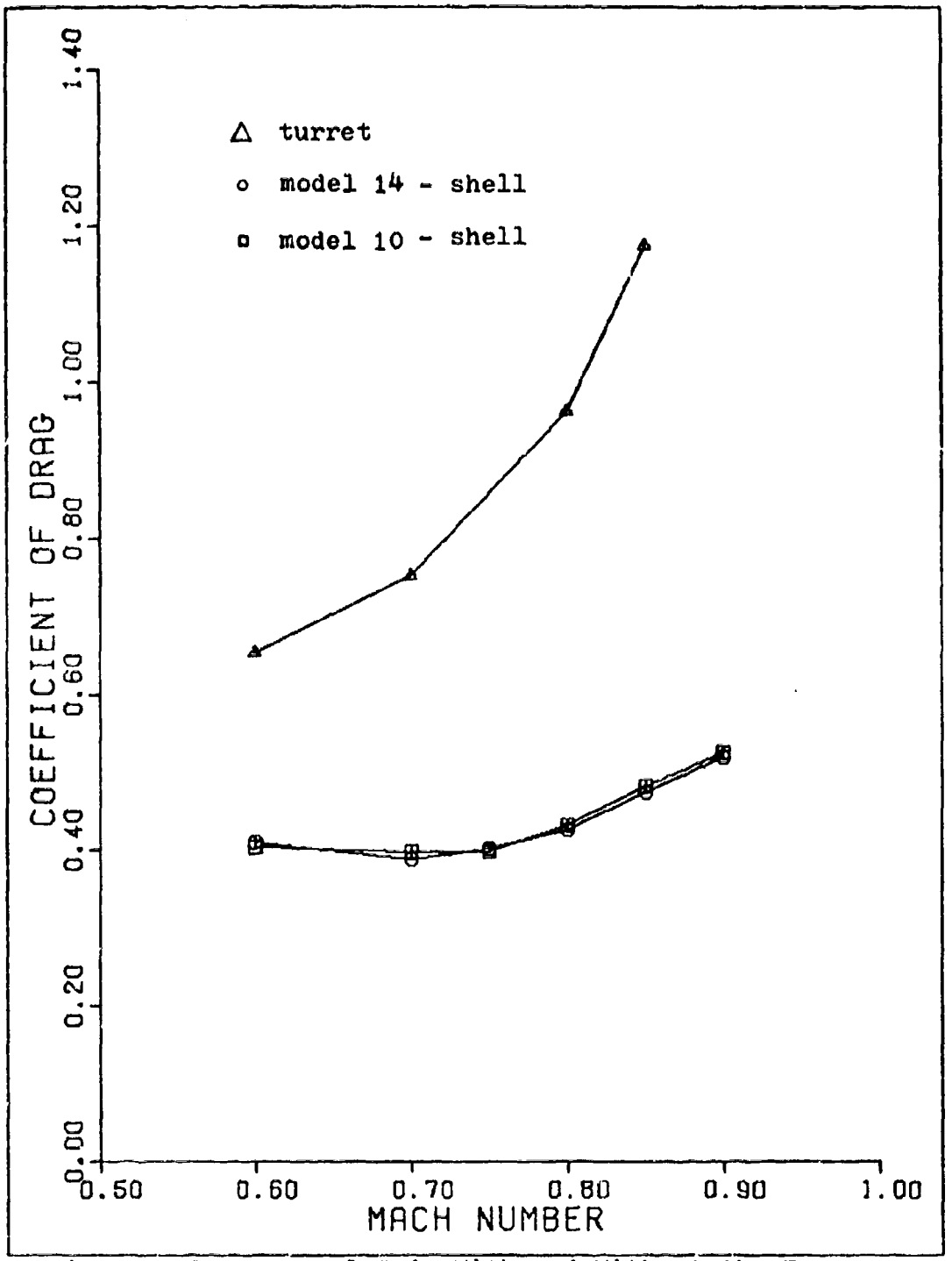

Fig. 9. Incremental C_D's With and Without the Force Balance Bridged by Tubes

The difference between the drag coefficients for these two models is the turret drag. The drag for the non-interference fairing, turret, and dorsal fin B is the difference between the two lines in Fig 11.

By calculating incremental drag coefficients, the drag contribution of each component was determined. The drag reduction due to the small side fairings and dorsal A can be seen in Fig 12. The addition of the small side fairings decreased the drag increment. Figure 13 shows the effect of dorsal fin B and the small side fairings on the drag increment. In combination with dorsal fin B the small side fairings increased the drag. As seen from these two graphs, model 6 reduced the drag on the bare turret the largest amount.

An interesting aspect of the incremental drag results is that the analysis of the cross-sectional area distribution did not predict the least drag design. This would indicate that the drag was influenced by local near field flow and simple far field area rule was not adequate to predict the drag.

The variation in drag as a function of Reynolds number can be seen in Figs 14 and 15. An increase of from 2×10^6 to 3×10^6 in Reynolds number/ft caused a significant increase in the incremental drag coefficient for model 6. But the same increase in Reynolds number caused a decrease in the drag coefficient for the bare shell, as predicted by the Prandtl-Schlichting turbulent

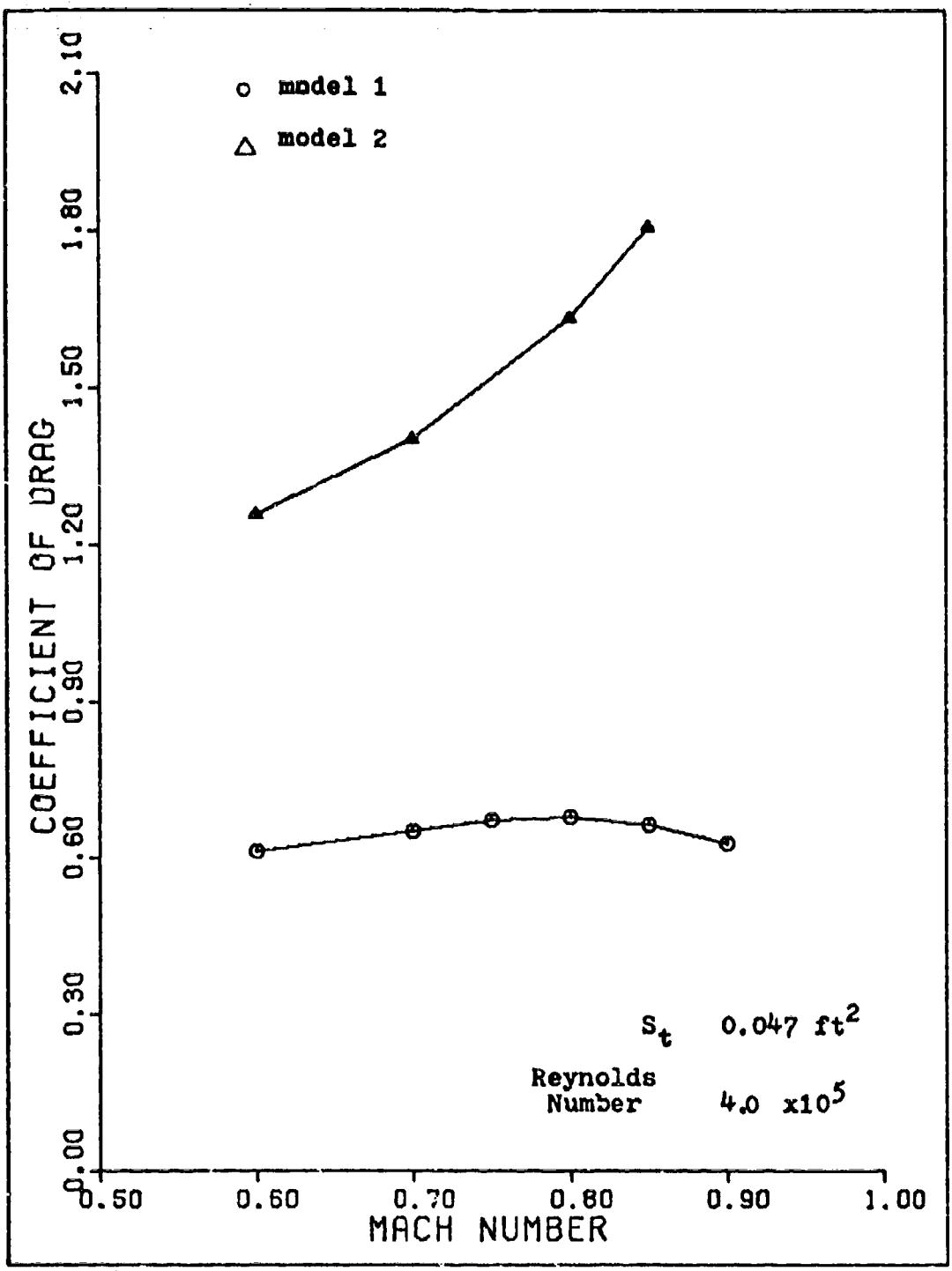

Fig. 10. Drag Coefficients versus Mach number for Models 1 and 2

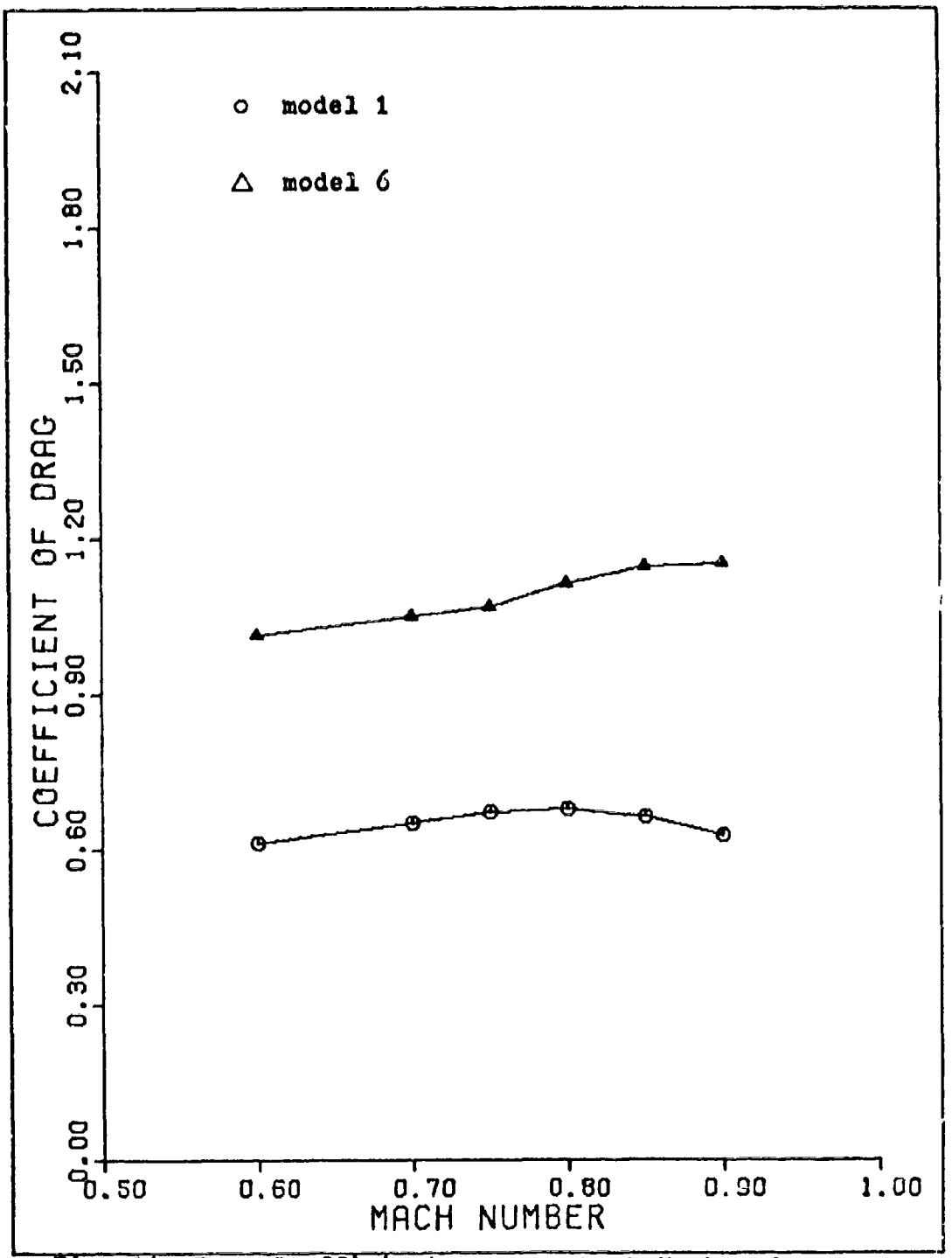

Fig. 11. Drag Coefficients versus Mach Number for Models 1 and 6

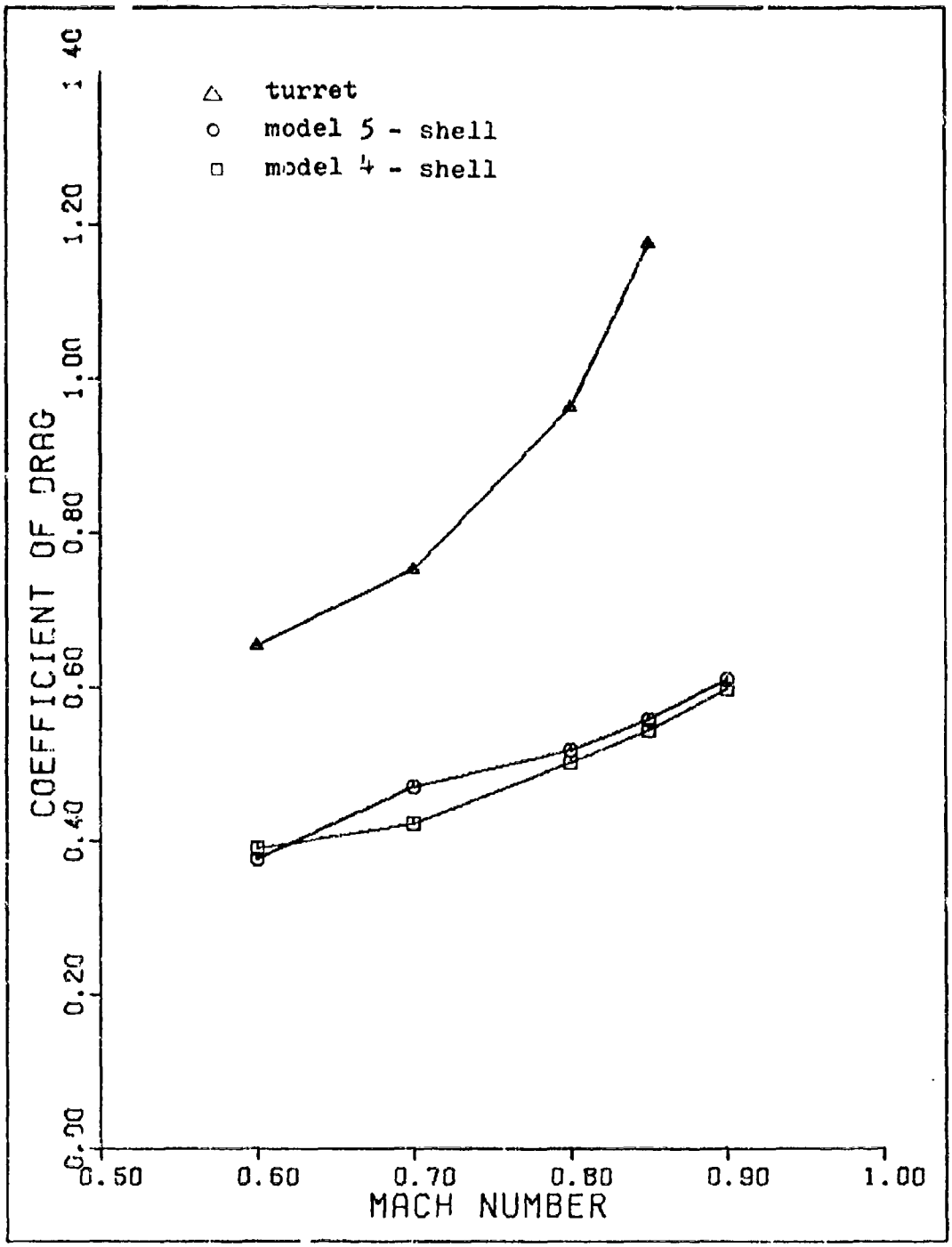

Fig. 12.Incremental C_D's as a Function of Configuration

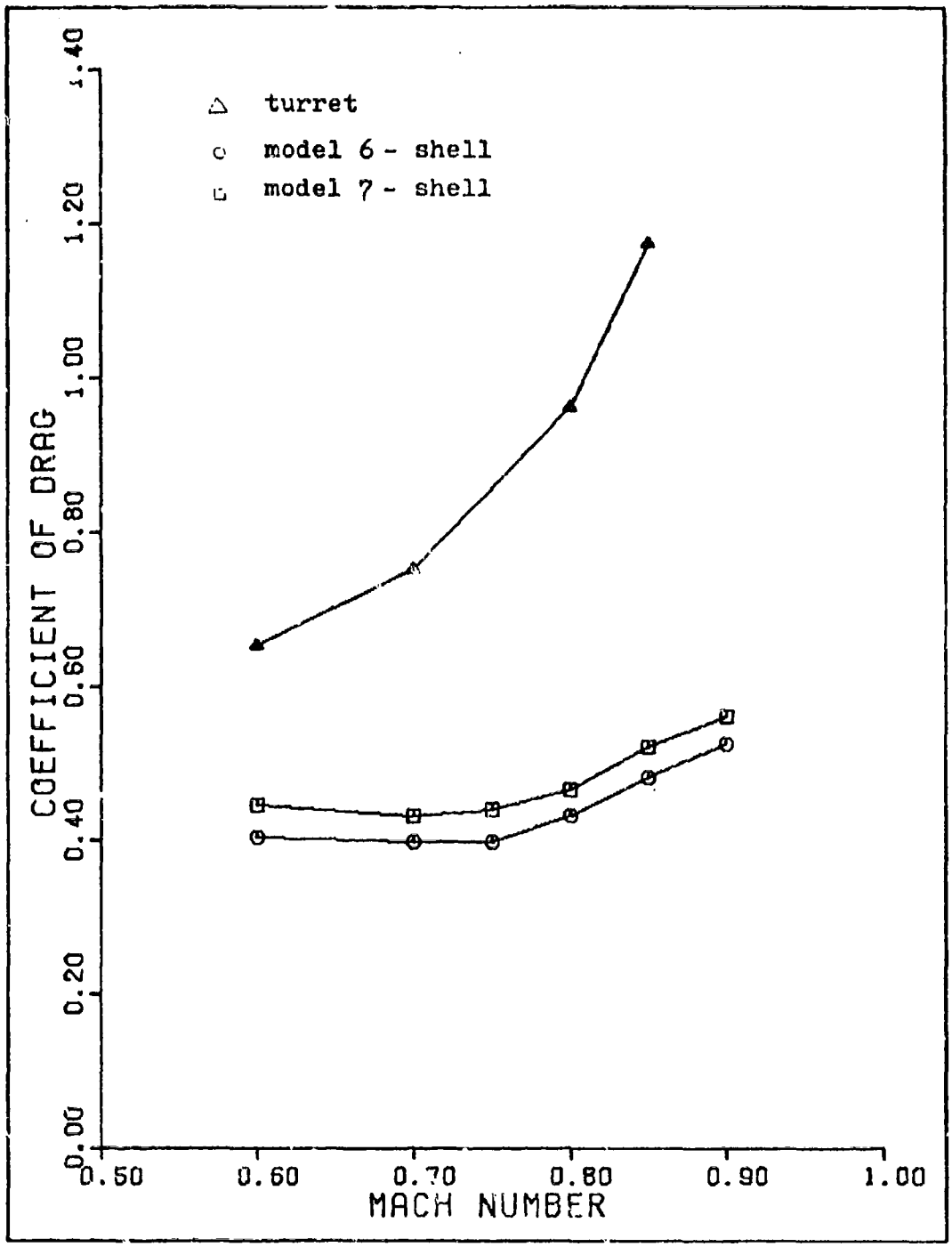

Fig. 13. Incremental C_D's as a Function of Configuration

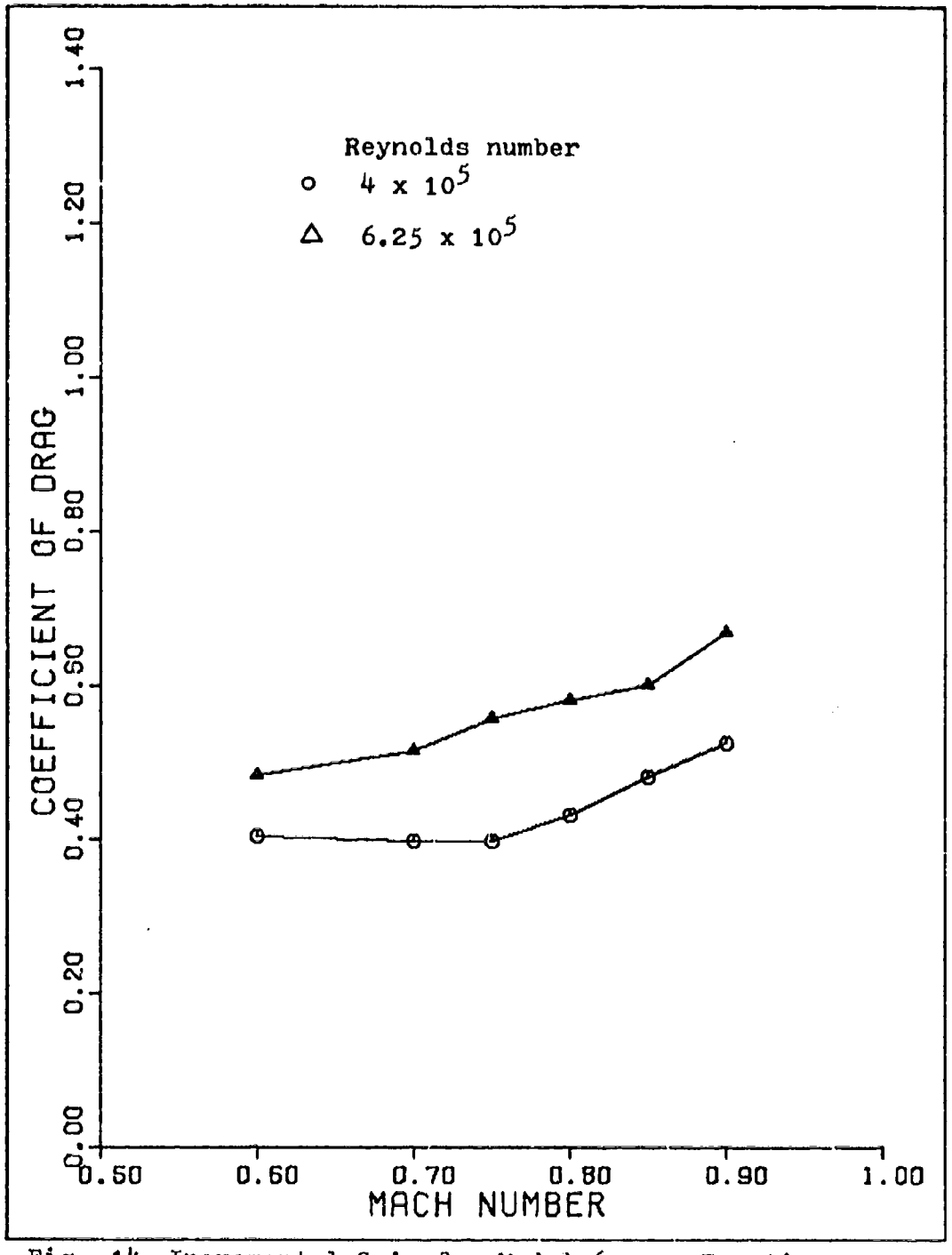

Fig. 14. Incremental C_D's for Model 6 as a Function of Reynolds Number

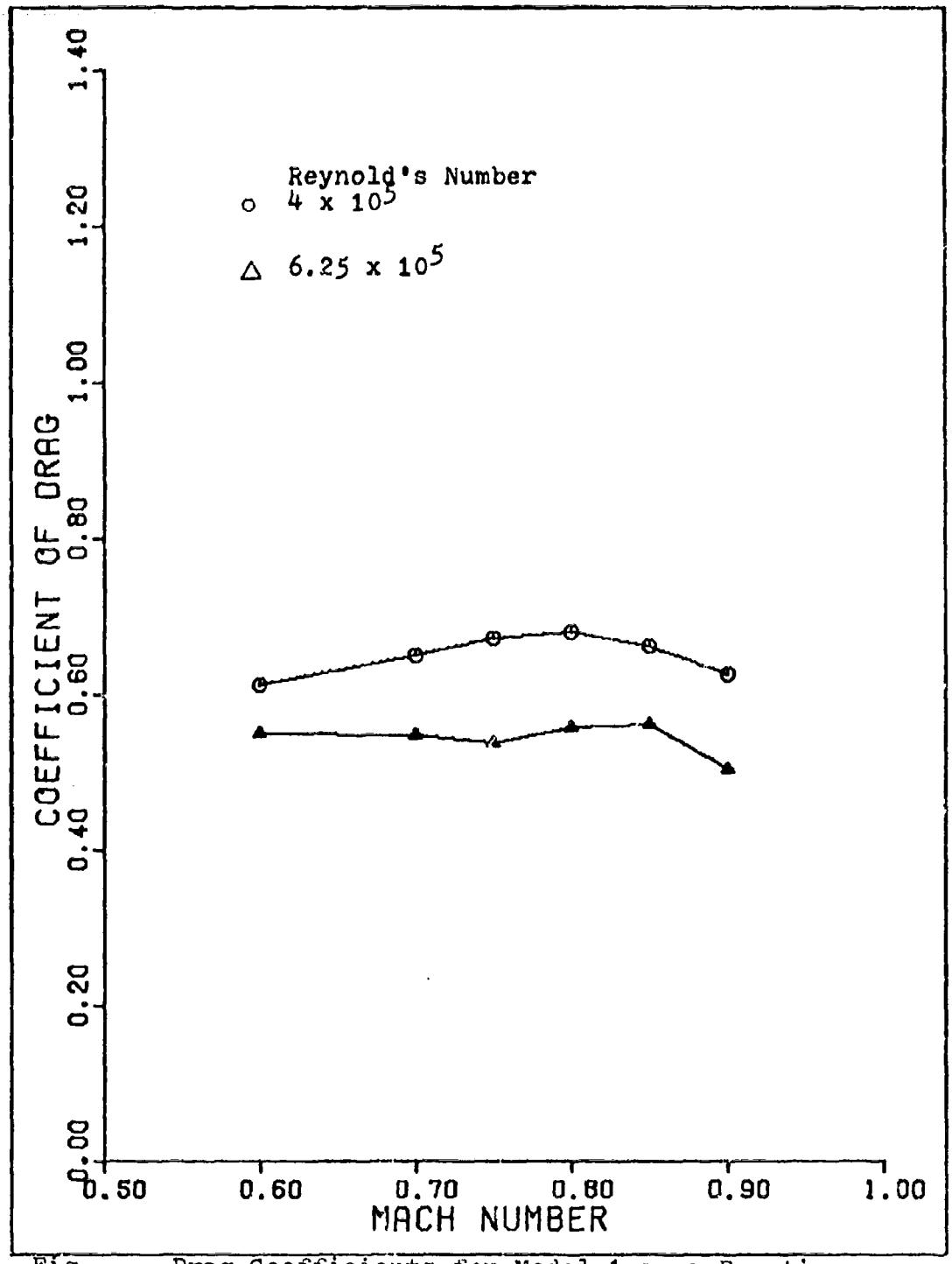

Fig. 15. Drag Coefficients for Model 1 as a Function of Reynolds Number

skin friction equation. This is further evidence that the flow field around the turret is complex and difficult to analyze.

Figure 16 shows the effect of elevation angle Δ2 on the drag coefficient. For increasing Mach number, the drag of model 8, Δ2-30°, approaches that of model 9, Δ2-15°.

Unsteady Pressures

The unsteady pressure measured by the transducer in the turret cavity was found to be the only one of significance. The PSD for the pressure in the cavity varied only slightly with changes in Mach number and configuration. The typical value of peak gains, in db, versus frequency for all configurations is given in Fig 17. The frequency range of 1600 to 1800 Hz always had the highest level of gain readings, which were between -10 and -30 decibels. The azimuth angle of the turret had an obvious effect. At an angle of 90°, the gain peaks in the range of 1600 to 1800 Hz disappeared. All the peaks had values of between -25 to -31 decibels in the frequency range of 100 to 1500 Hz. A typical PSD for 90° is given in Fig 18.

The effect of turret angle on cavity pressures can be seen better in the plots of P_{rms} for the cavity versus azimuth angle Δ1, Fig 19 and 20. The large values of P_{rms} for model 12 for angles of 0° to 30° are due to flow being disturbed by the side fairings

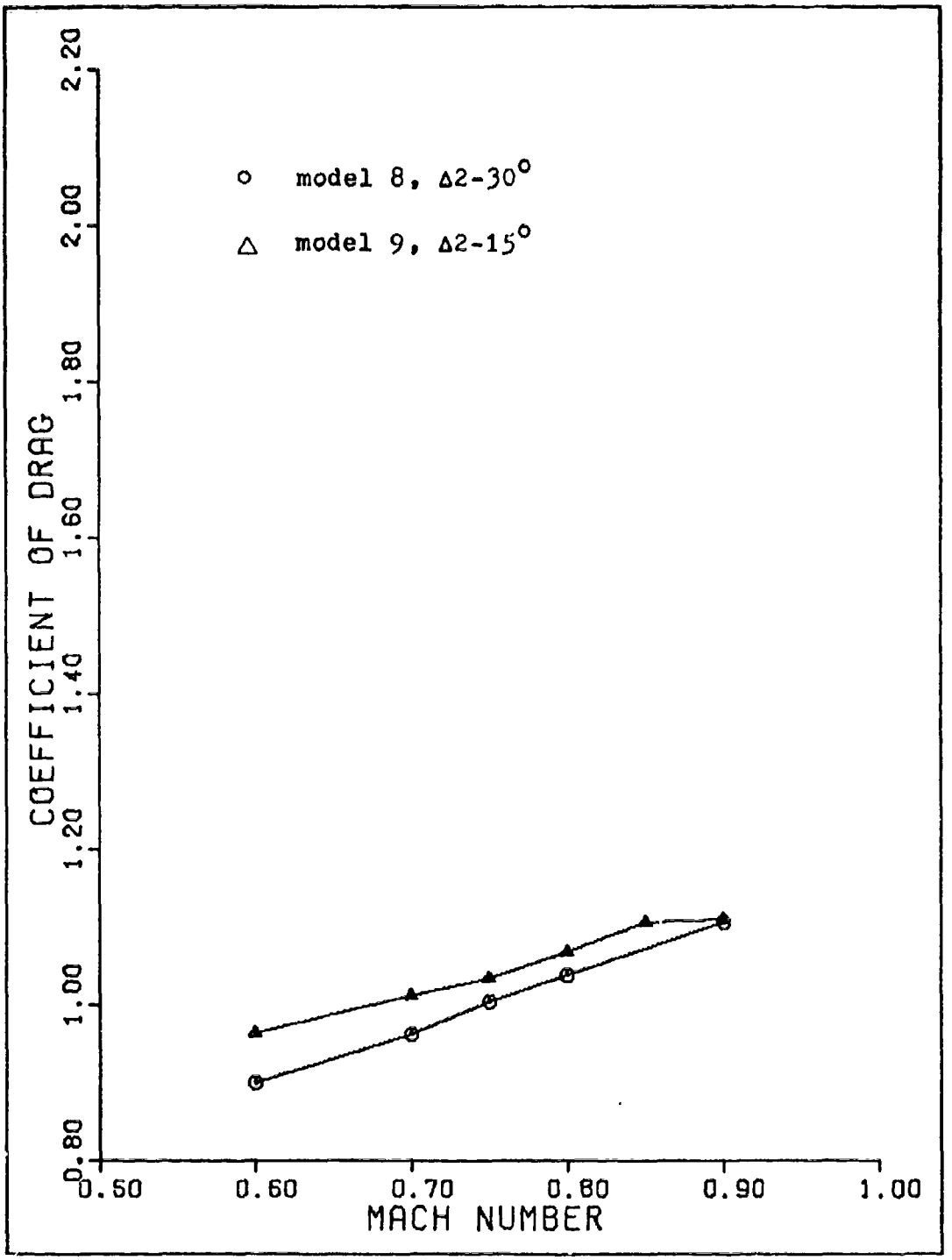

Fig. 16. Drag Coefficients as a Function of Turret Elevation angle, Δ2

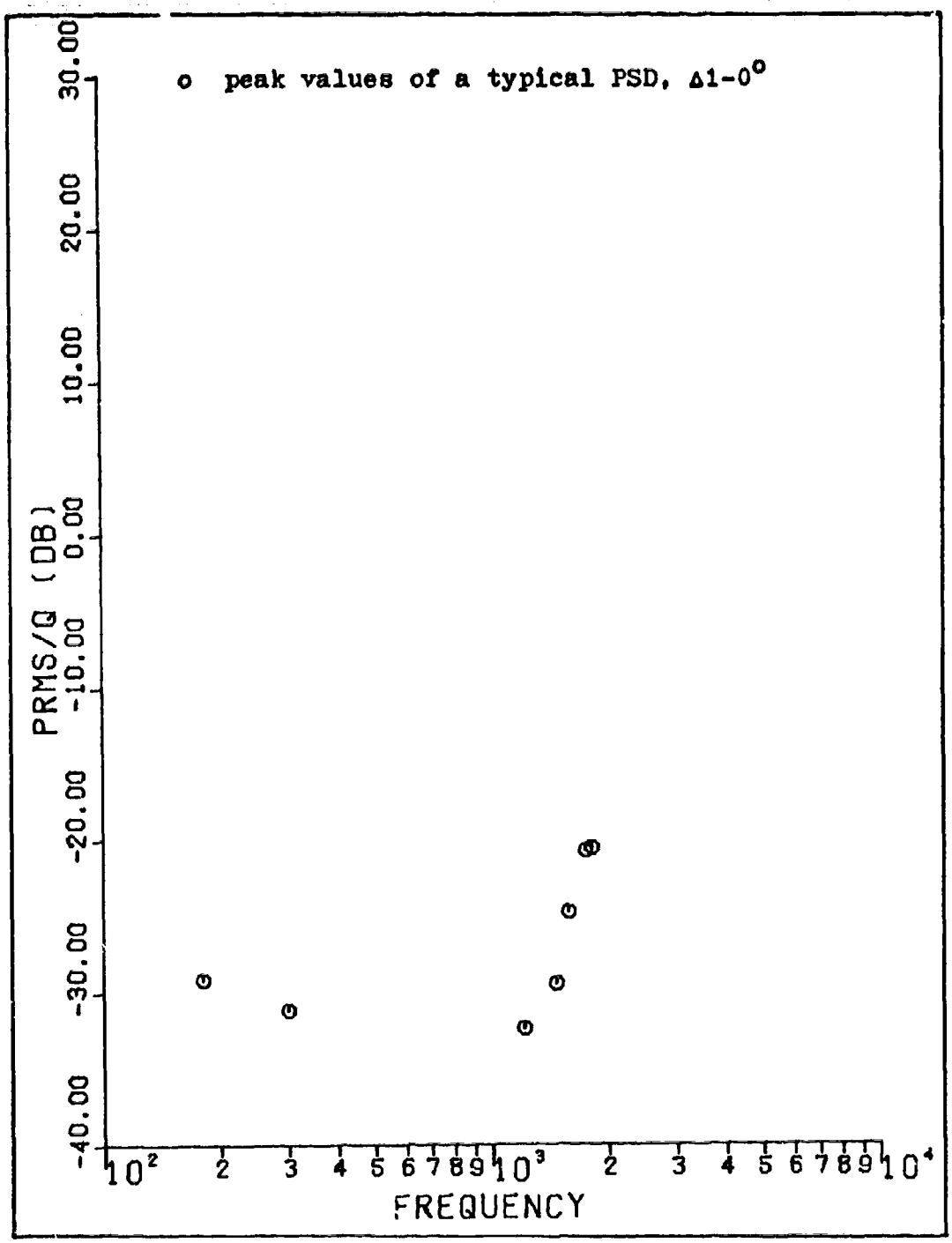

Fig. 17. A Power Spectral Density Representative of All Models

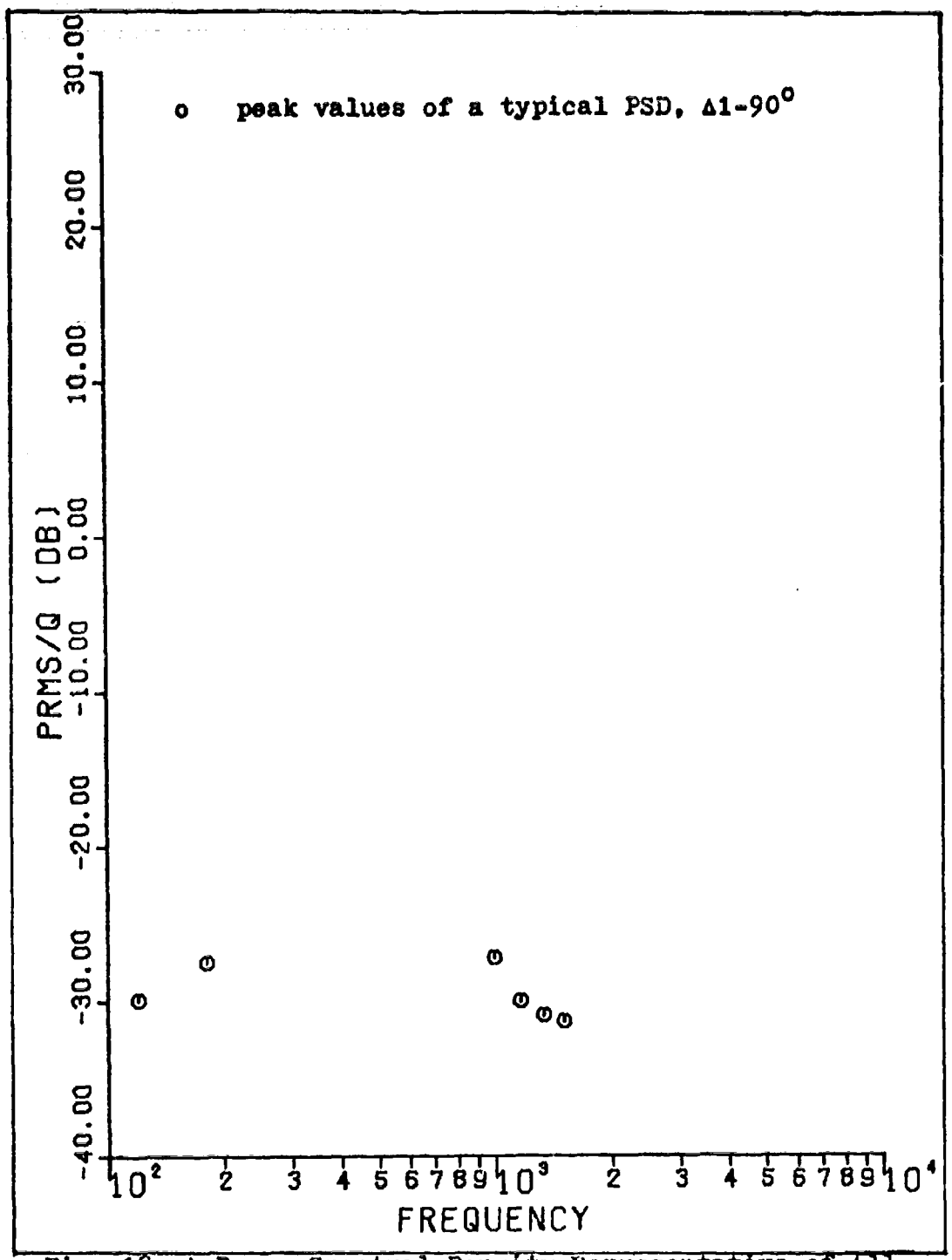

Fig. 18. A Power Spectral Density Representative of All Models

and impinging on the cavity opening. Model 10 without the side fairings has considerably smaller values for all Mach numbers tested. The large spike at 50° and Mach 0.6 for model 12 is probably due to the particular geometry of the cavity. The flow is disturbed by the forward lip and at 50° impinges directly on the rear lip on the cavity creating a large resonance condition as indicated by the PSD given in Fig 20.

Figure 19 shows that model 6 is also the best design from the standpoint of the smallest values of P_{rms} in the cavity at all Mach numbers. Rotating the cavity to 15° and 30° of elevation angle did not significantly change the shape of the P_{rms} versus $\Delta 1$ curve.

The general effect of increasing Reynolds number is to increase the magnitude of the P_{rms}/q peaks but for the values of $\Delta 1$, at which the peaks occurred, to remain the same. Figure 21 shows the difference between test runs with Reynolds number/ft of 2×10^6 and 3×10^6.

Steady Pressures

The survey of static pressure orifices along the model was almost constant for variations in Mach number, azimuth and elevation angles of the model. The only variations in the pressure distribution was an increase in the static pressure in the region of stagnation flow in front of the turret and in the area behind the aft fairing for increases in Mach number, Figs 22 and 23.

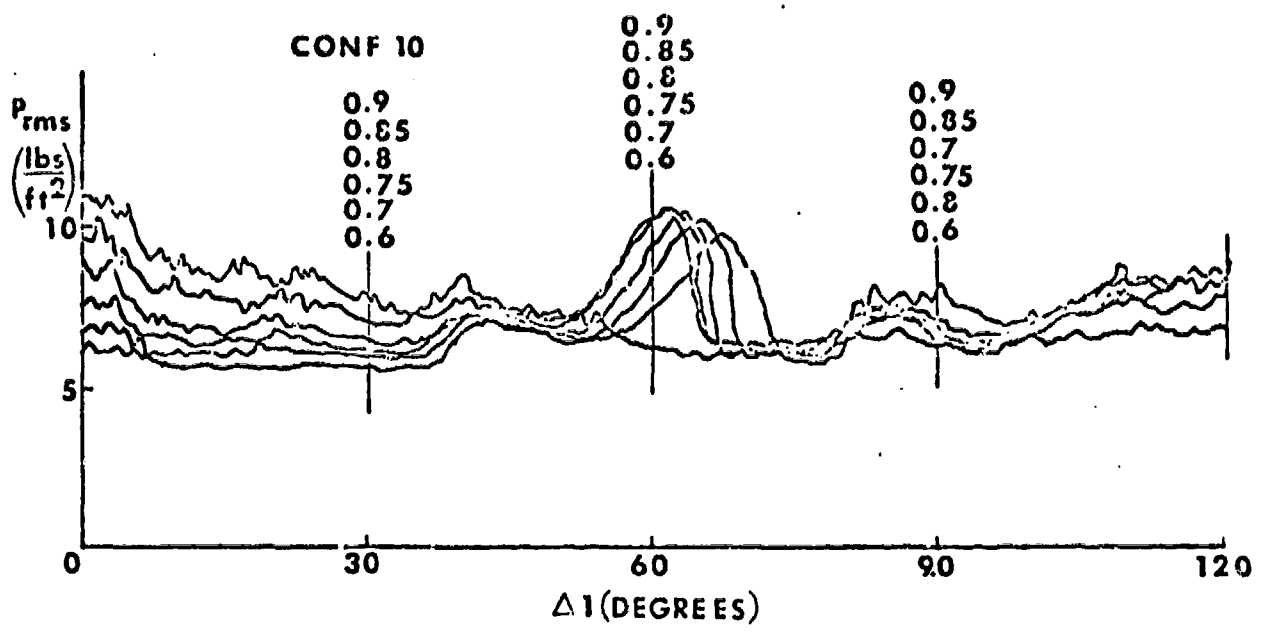

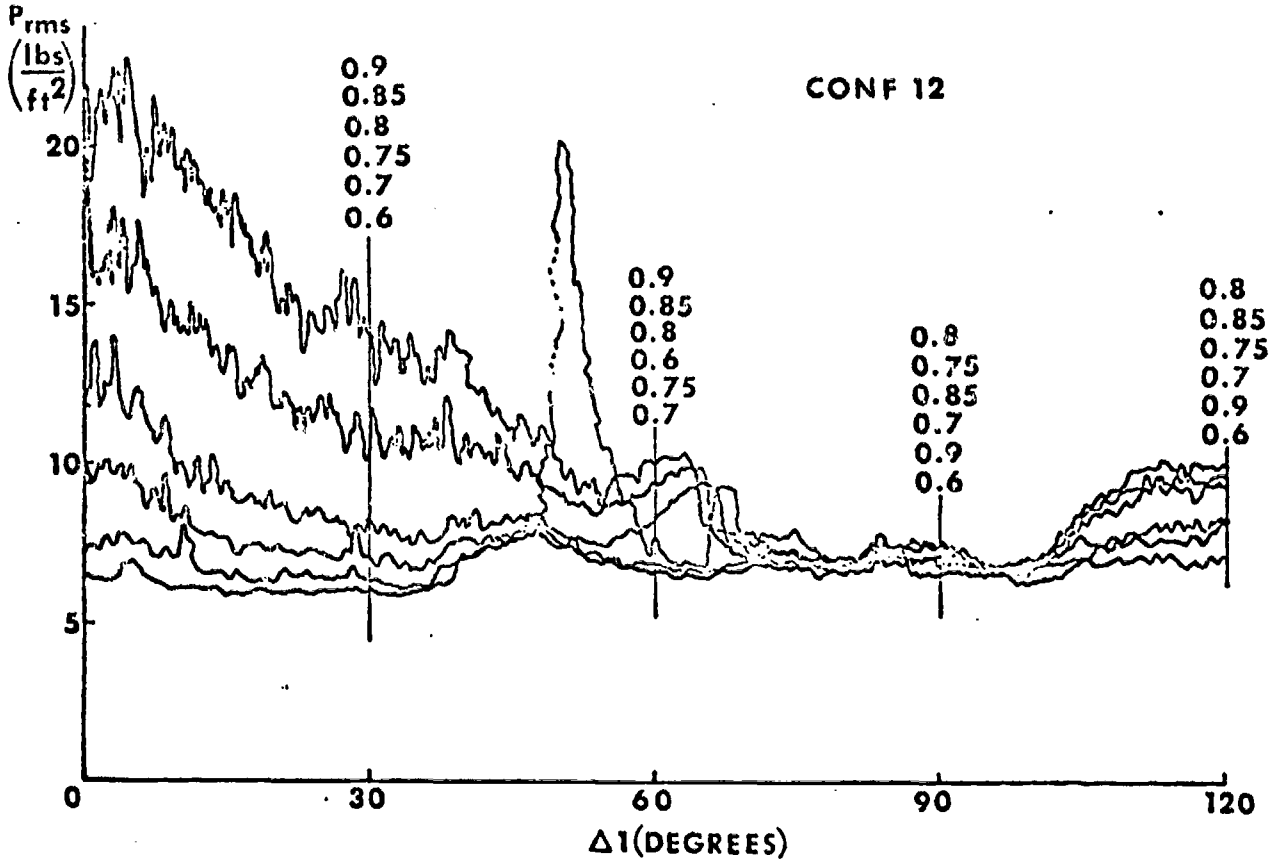

Fig. 19. Turret Cavity Readings of Models 10 and 12 for Varying Mach Numbers and Turret Angle, Δ1

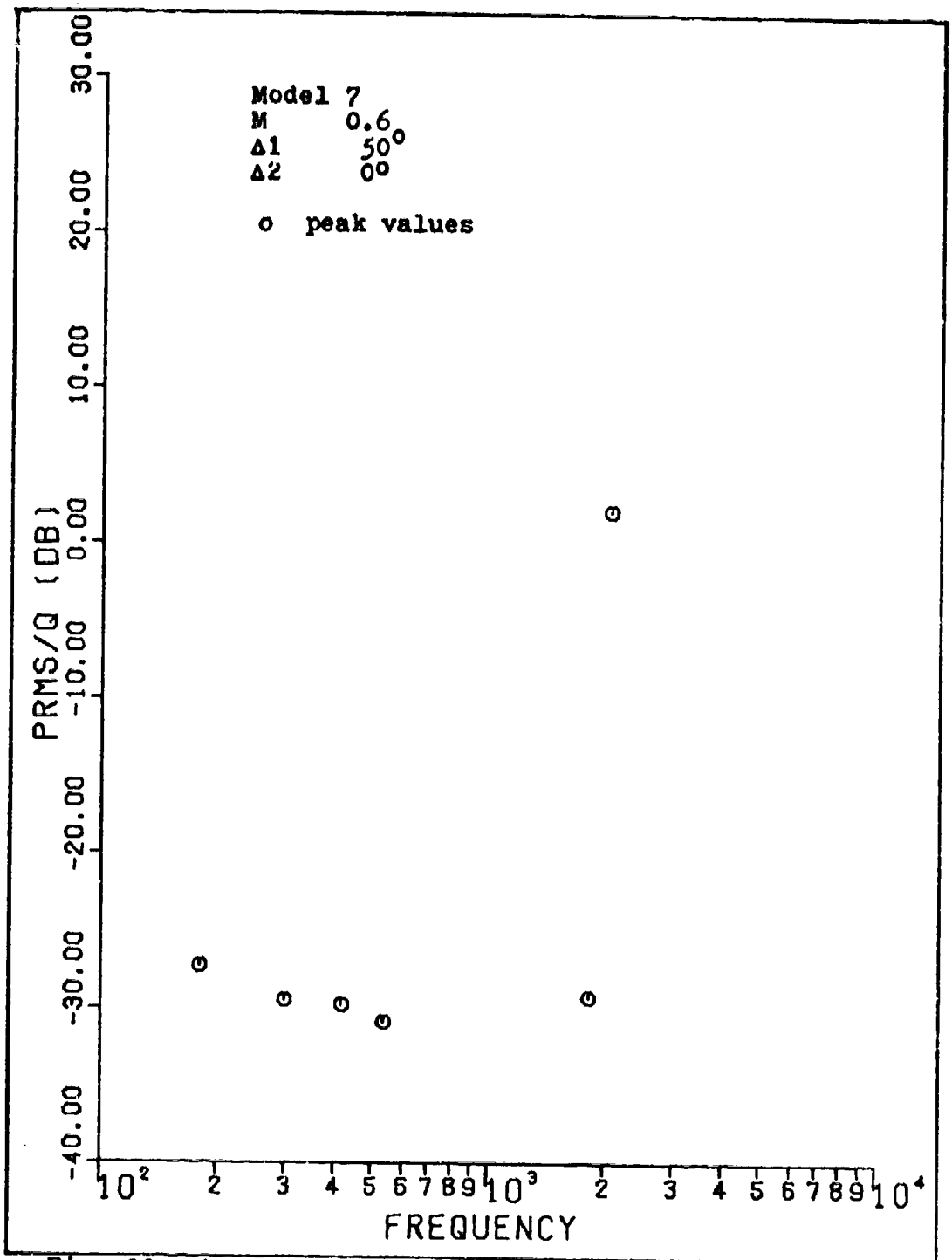

Fig. 20. The Most Significant Power Spectral Density Graph

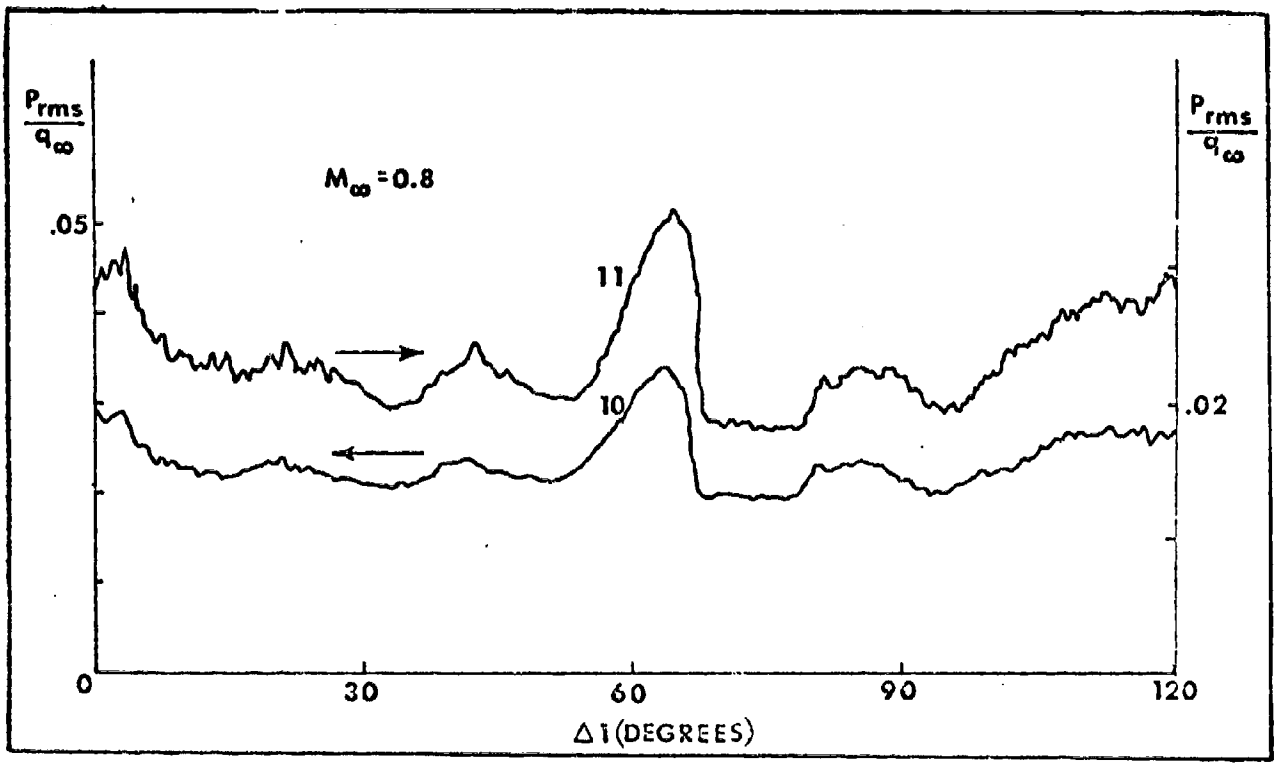

Fig. 21. Reynolds Number Effects on the Pressure Fluctuation in the Turret Cavity as a Function of Azimuth Angle, Δ1

Oil Flow

For model 6, the effect of increasing Mach number on the oil flow was to move the line of flow separation forward on the turret, Fig 24. Adding the side fairings to model 6, changed the flow around the model very little. The only change was an appearance of a vortex at the base of the turret. This vortex grew in size and moved forward on the turret with increasing Mach number, Fig 25.

The flow over the rest of the model was independent of changes in Mach number. The drawings from the oil flow tests are in Appendix C.

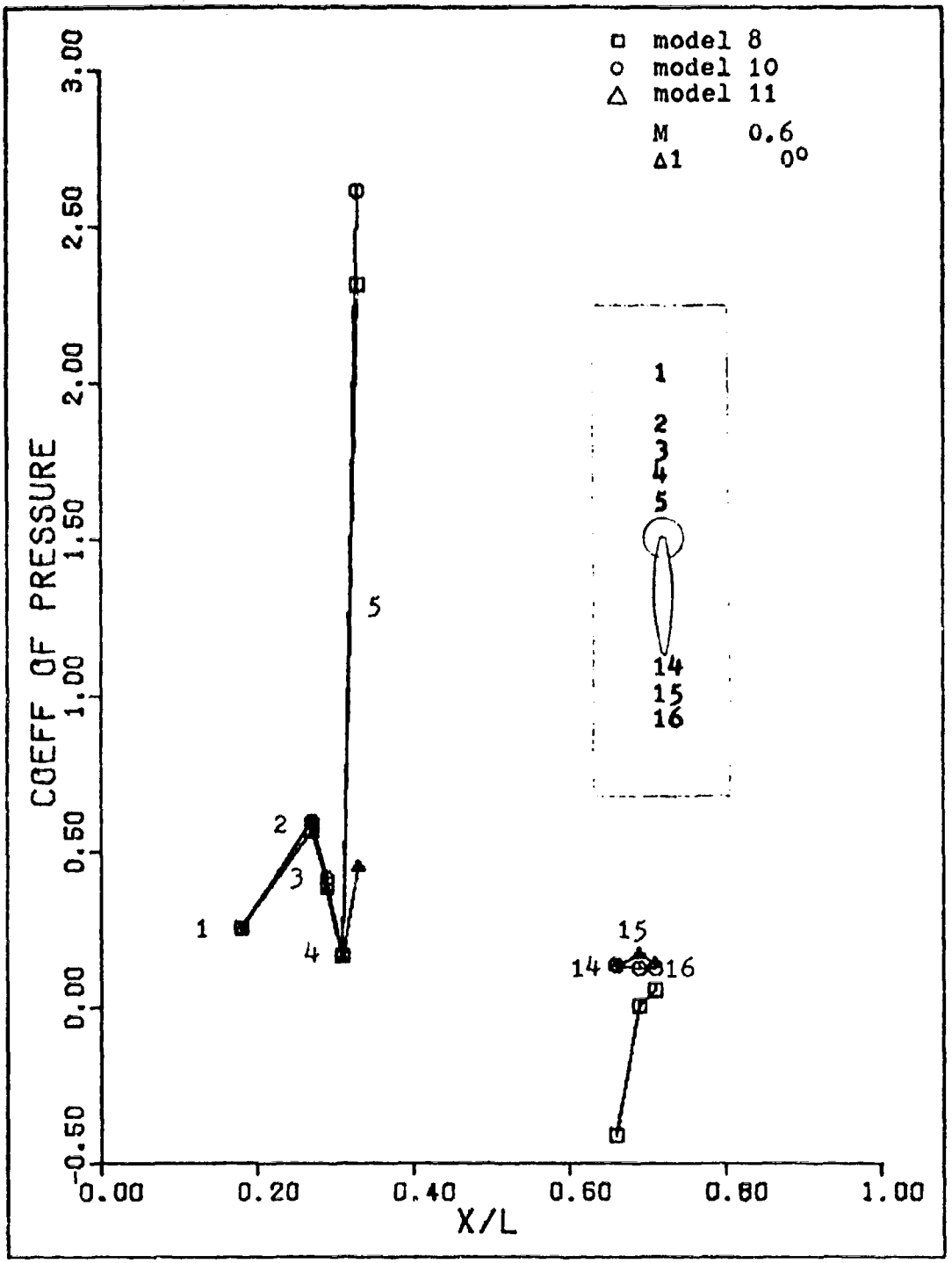

Fig. 22. Pressure Distribution as a Function of Position and Configuration

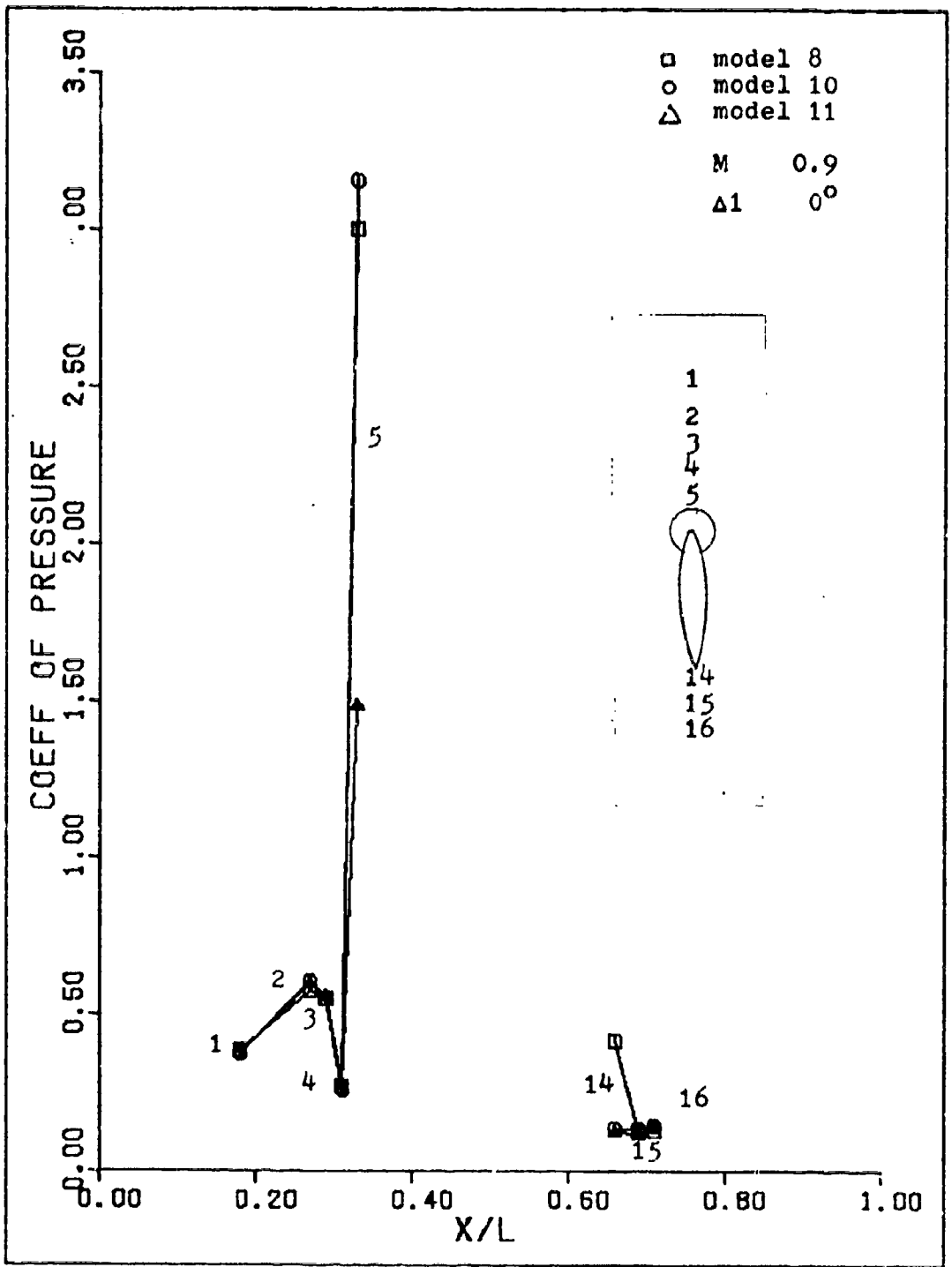

Fig. 23. Pressure Distribution as a Function of Position and Configuration

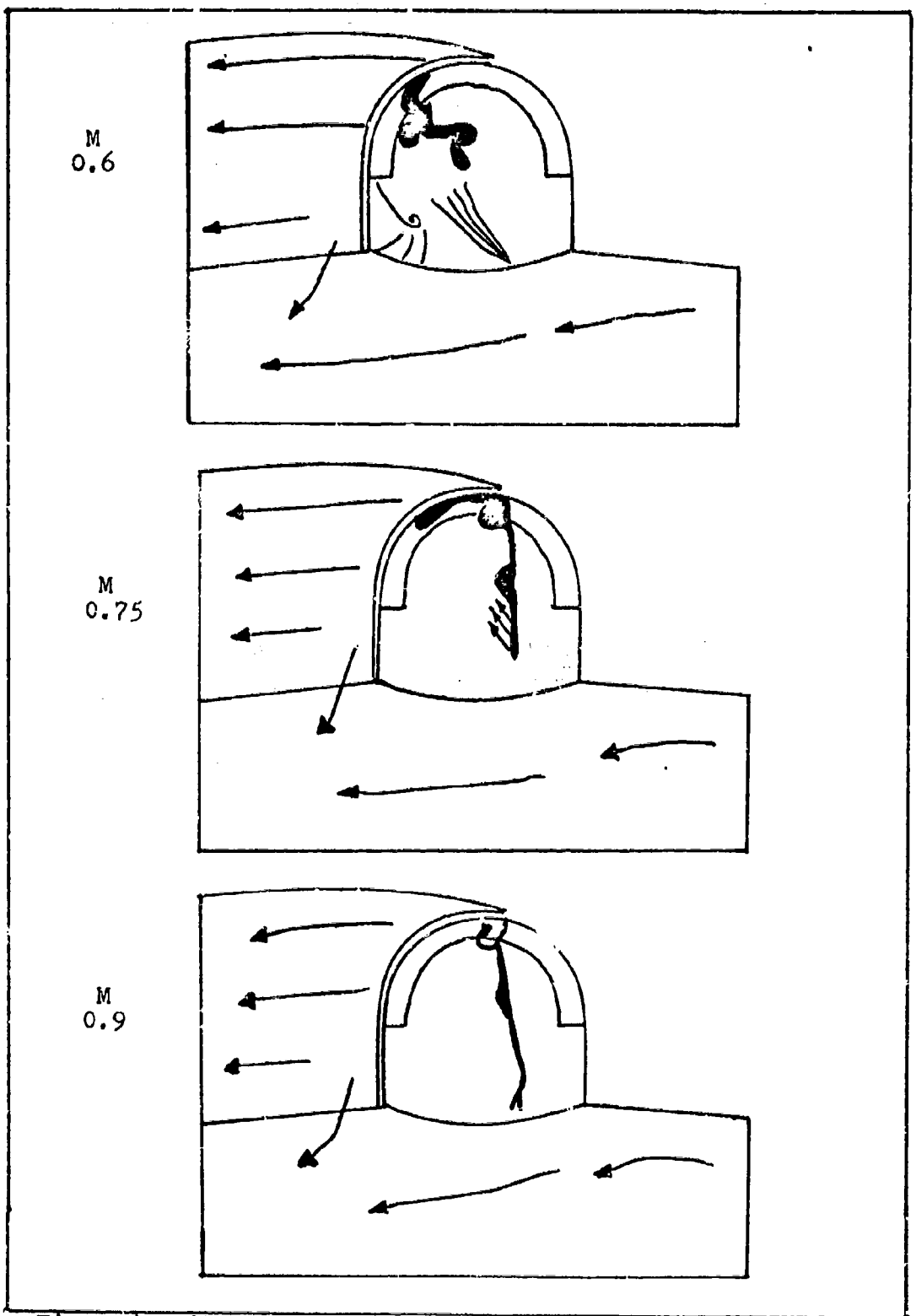

Fig. 24. Oil Flow Patterns on the Turret for Model 6

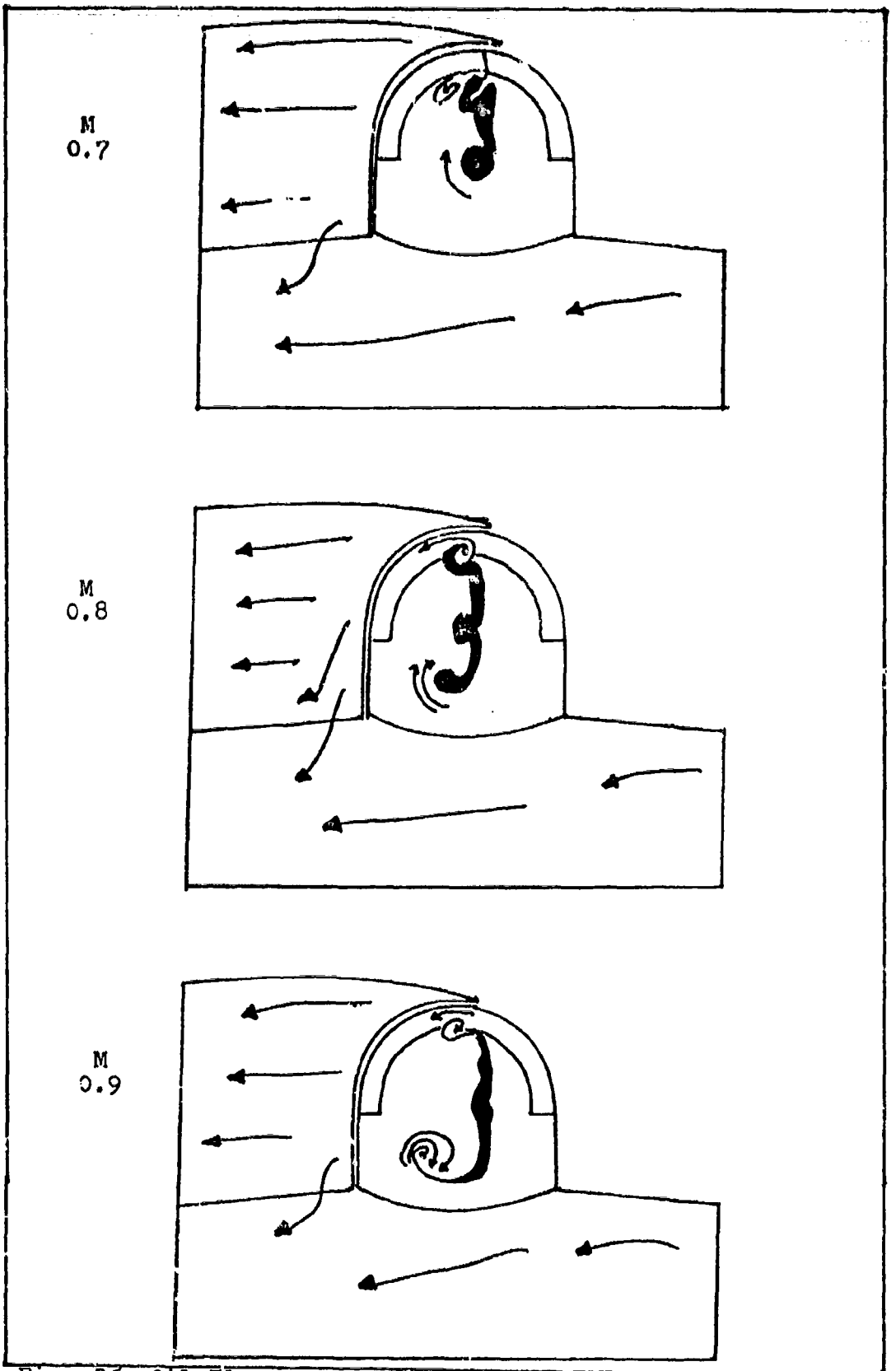

Fig. 25. Oil Flow Patterns on the Turret for Model 7

V. Conclusions and Recommendations

Conclusions

The results of this test confirm the findings by Dr. Van Kuren during his tests at the United States Air Force Academy. Of all the configurations tested, model 6 had the least drag. The reduction in incremental drag for a bare turret by the placement of dorsal fin B aft of the turret was as much as 55% of the bare turret drag, Fig 9. This compares with a 50% reduction achieved by Dr. Van Kuren using a similiar fairing.

The use of side fairings to reduce the drag was successful on models 3 and 4 but unsuccessful on model 7. This indicates a three dimensional flow effect between all the fairings that influenced the total drag. Also, the local area distribution could not be used to determine the optimum design tested. There appeared to be some correlation between the drag on models 3, 4, and 5 and their area distributions but this relationship could not be carried over to model 6 and 7. The configurations with side fairings had larger pressure fluctuations in the turret cavity than those without side fairings. This appeared to be due to the shedding of turbulent flow from the forward fairings into the cavity. In fact, the only significant resonance condition was probably due to the unique geometry of the cavity, Fig 18. With the turret at an angle of 50^{o}, turbulent flow from the side fairings passed directly

over the front lip of the cavity and impinged directly on the rear lip causing a resonance condition. This resonance level had not been experienced in previous testing. Therefore, it is believed to be due to the unique dimensions and geometry of this model. Future designers should be aware of this condition.

Comparing the test data taken at the two different Reynolds numbers, confirms the fact that the transonic flow field around the model is a very complex one. This indicates the empirical analysis is the only method available to determine the optimum design for drag reduction of a particular model.

Recommendations

Further testing of configuration 6 is recommended. The testing should be conducted with a stiff force balance and in a high Reynolds number transonic facility. The results of the additional testing should be used to validate the results of this test and to aid extrapolation of the drag data to where it could apply directly to flight testing of a full scale model. The additional testing should also include schlieren photographs of the model to locate shock waves on the turret and aft fairing. The schlieren system could not be used during this test because of the slotted walls in the test section.

Additionally, the data acquisition system for this test should be expanded. The system was limited in capability due to the conputer software program. It should be modified and expanded to handle any type of wind tunnel testing and degree of data acquisition. All the essential components of the system are present but the computer software program needs to be made general enough to handle any conceivable test. This would help change the job of the project engineer from one of data reduction to data analysis.

Bibliography

1. Gaudet, L., and K. Winter. Measurements of the Drag of Some Characterestic Aircraft Excrescences Immersed In Turbulent Boundary Layers. Technical Memo Aero 1538. London, England: Royal Aircraft Establishment, September 1973. (AD 918999)

2. Van Kuren, J., and W. R. Connor. Transonic Ten-Pin Tests Phase II Configuration Studies and Pressure Fluctuations. AFFDL FX-TM-73. Wright Patterson Air Force Base, Ohio: Air Force Flight Dynamics Laboratory, April 1973.

3. -----. Fairing Design for Fuselage Mounted Turret in Transonic Flow. AFFDL TM-73-115 FXM. Wright Patterson Air Force Base, Ohio: Air Force Flight Dynamics Laboratory, September 1973.

4. White, H. L. Trisonic Gasdynamic Facility Users Manual. AFFDL TM-73-82 FXM. Wright Patterson Air Force Base, Ohio: Air Force Flight Dynamics Laboratory, June 1973.

5. Icardi, Stephar E. An Experimental Investigation of Transonic Flow Around a Nose Section with an Off-Axis Longitudinal Cavity. Unpublished thesis. Wright Patterson Air Force Base, Ohio: Air Force Institute of Technology, December 1973.

6. Goethert, B. H. Transonic Wind Tunnel Testing. New York, New York: Pergamon Press, Inc., 1961.

7. Pope, A. Wind Tunnel Testing. New York, New York: John Wiley & Sons, Inc., 1954.

Appendix A

Model Configurations

This Appendix contains Figures 24 thru 33 which illustrate the various model configurations utilized in the experiment.

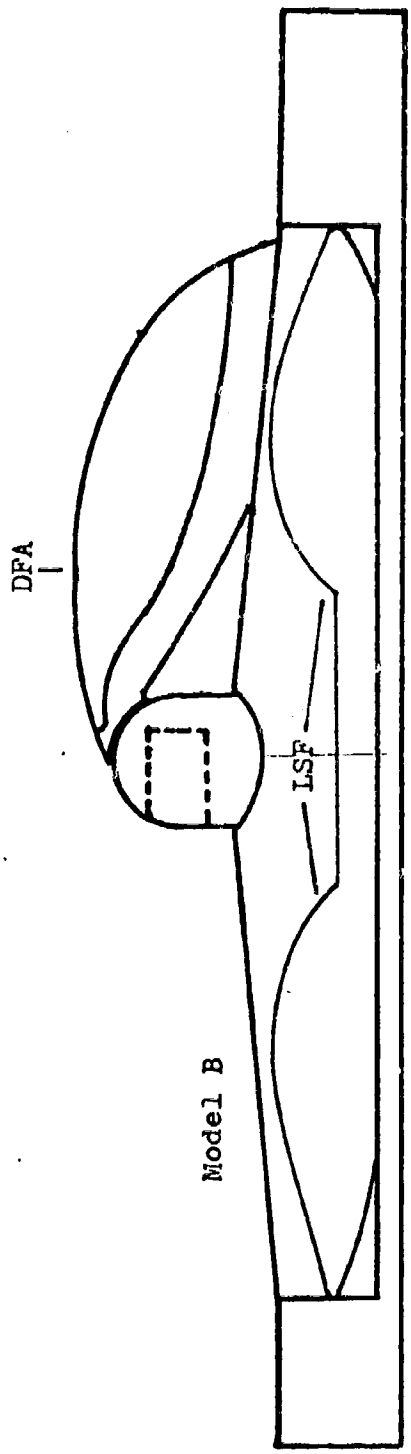

Fig. 26. Side View of Model 3

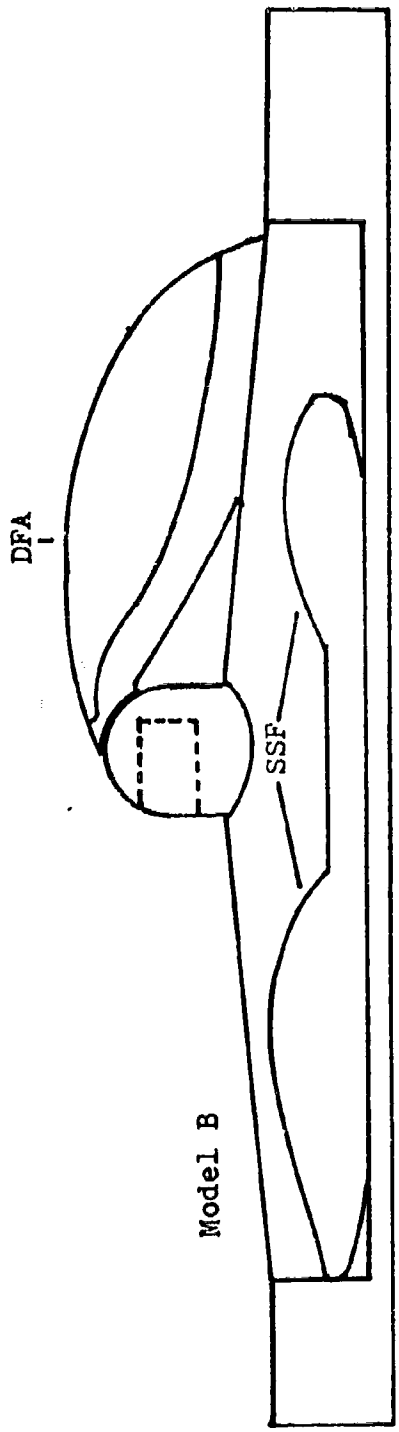

Fig. 27. Side View of Model 4

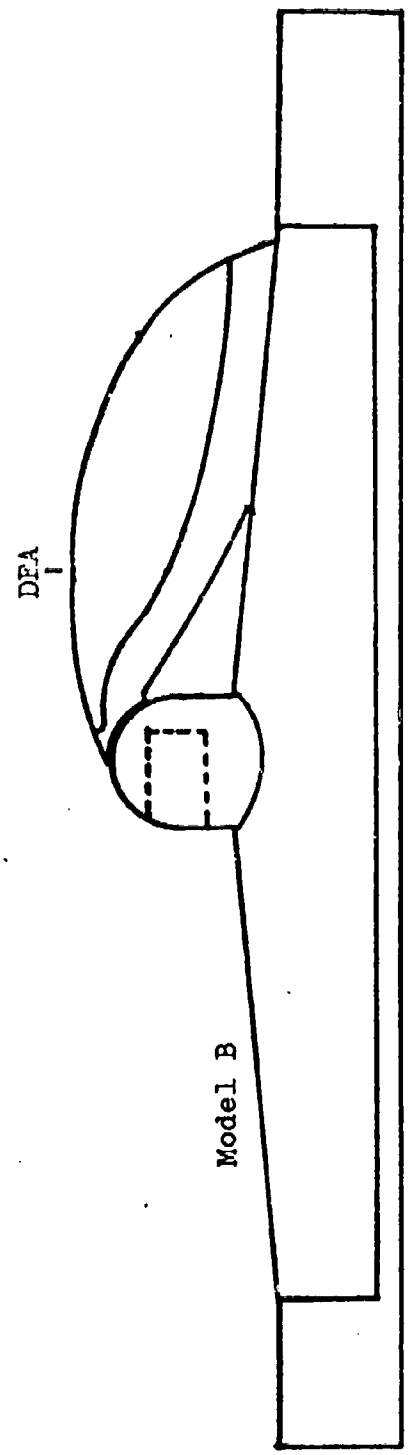

Fig. 28. Side View of Model 5

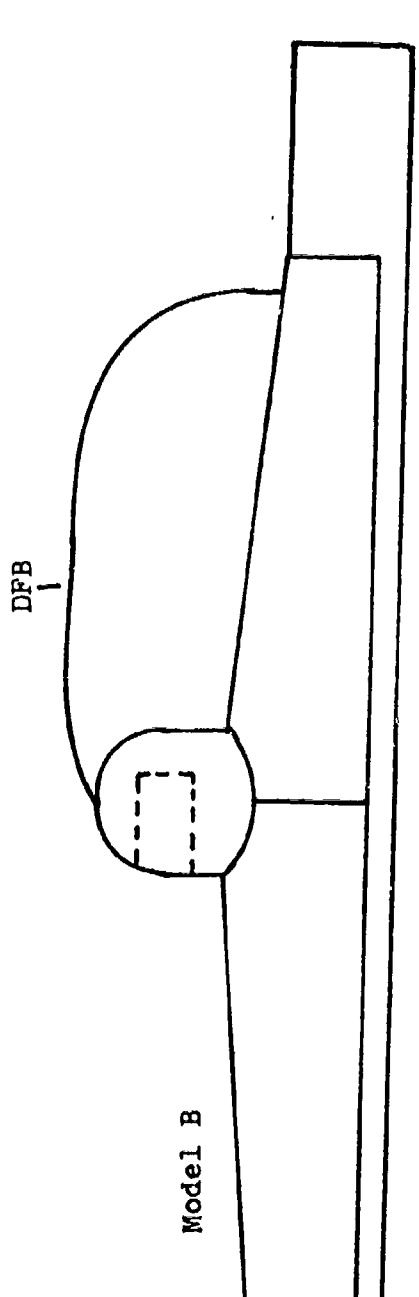

Fig. 29. Side View of Model 6

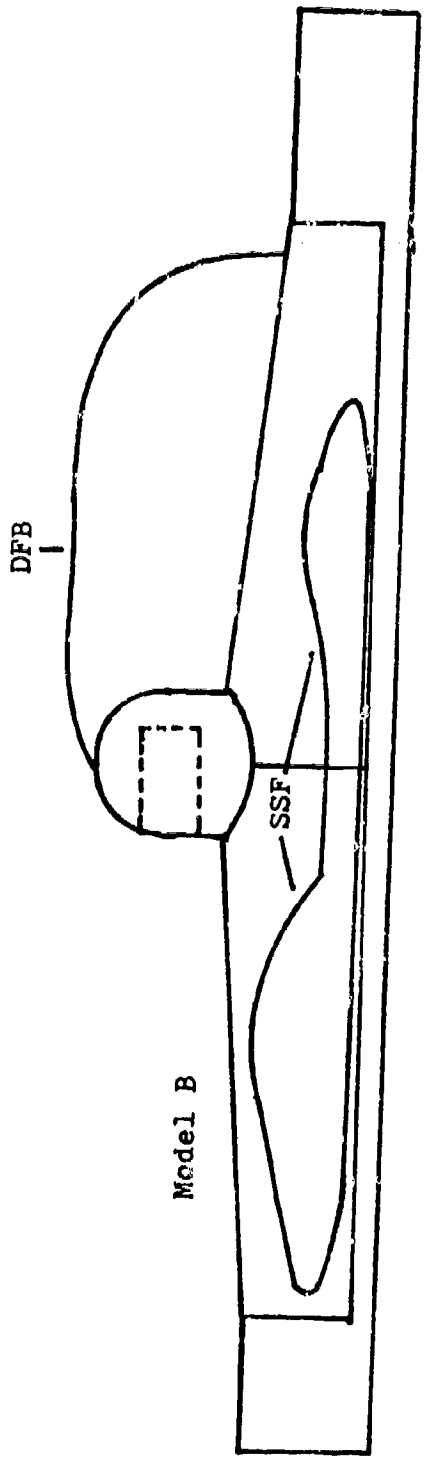

Fig. 30. Side View of Model 7

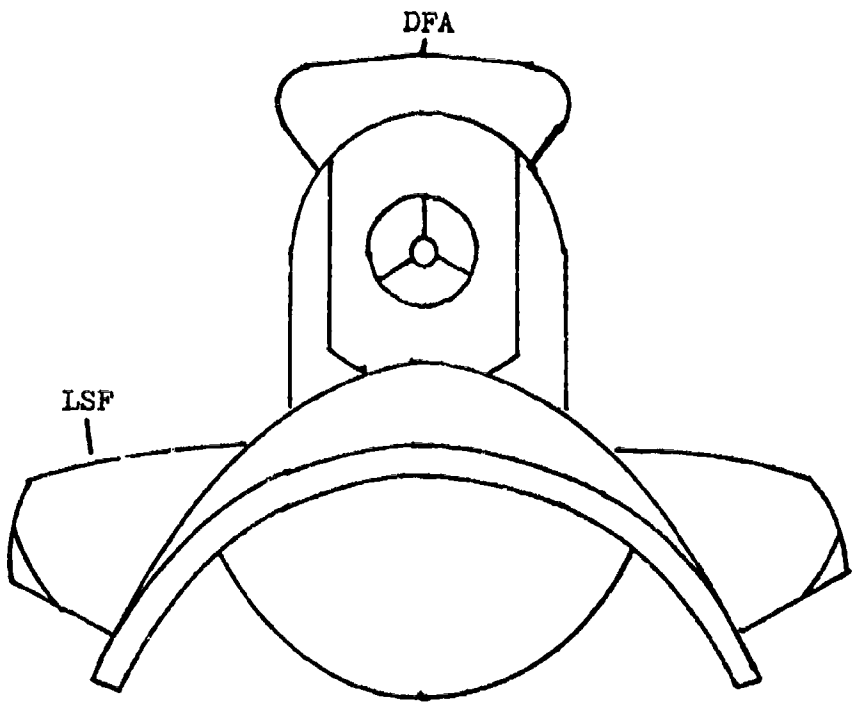

Fig 31. Front View of Model 3

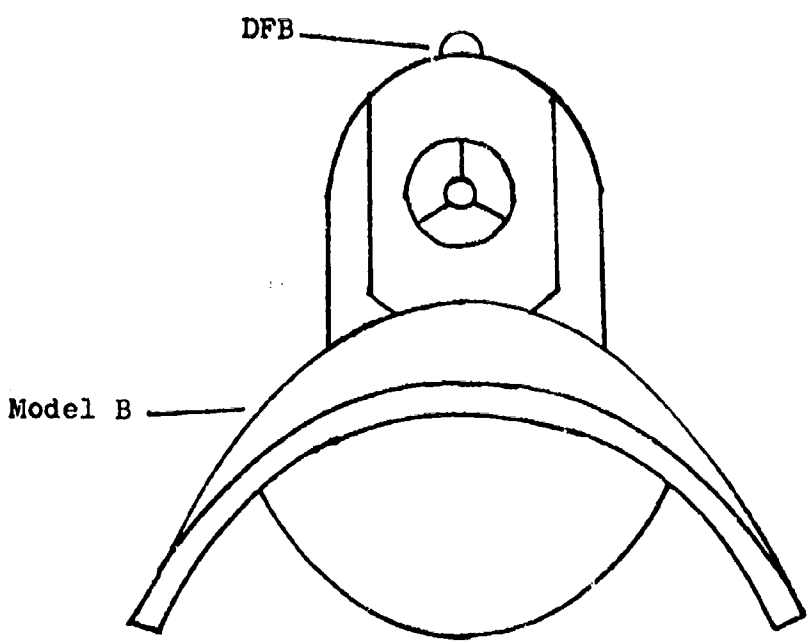

Fig. 32. Front View of Model 6

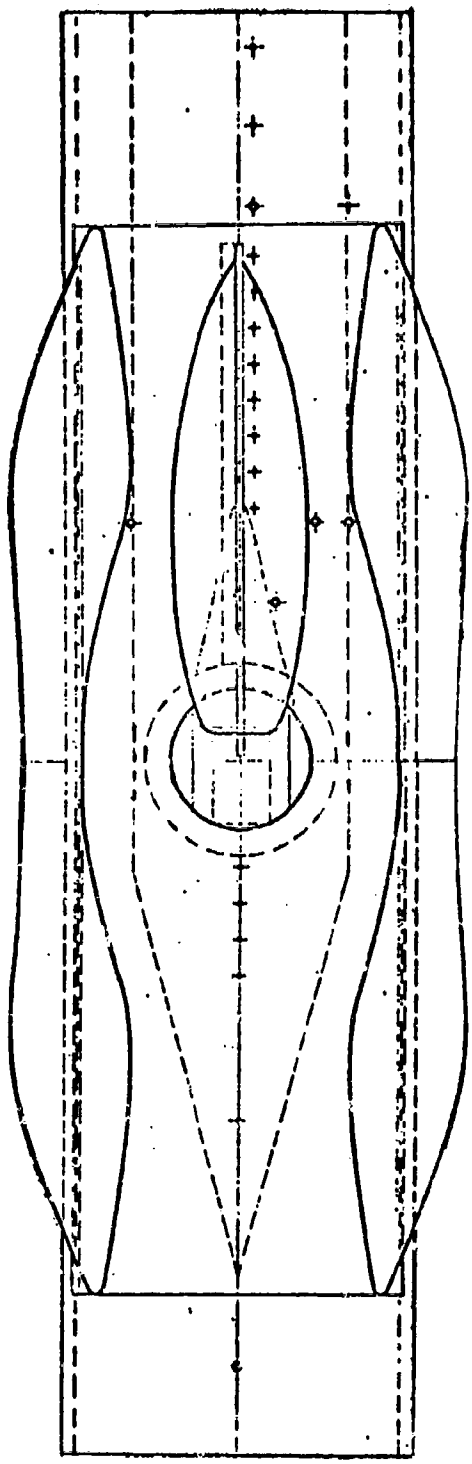

Fig. 33. Top View of Model 3

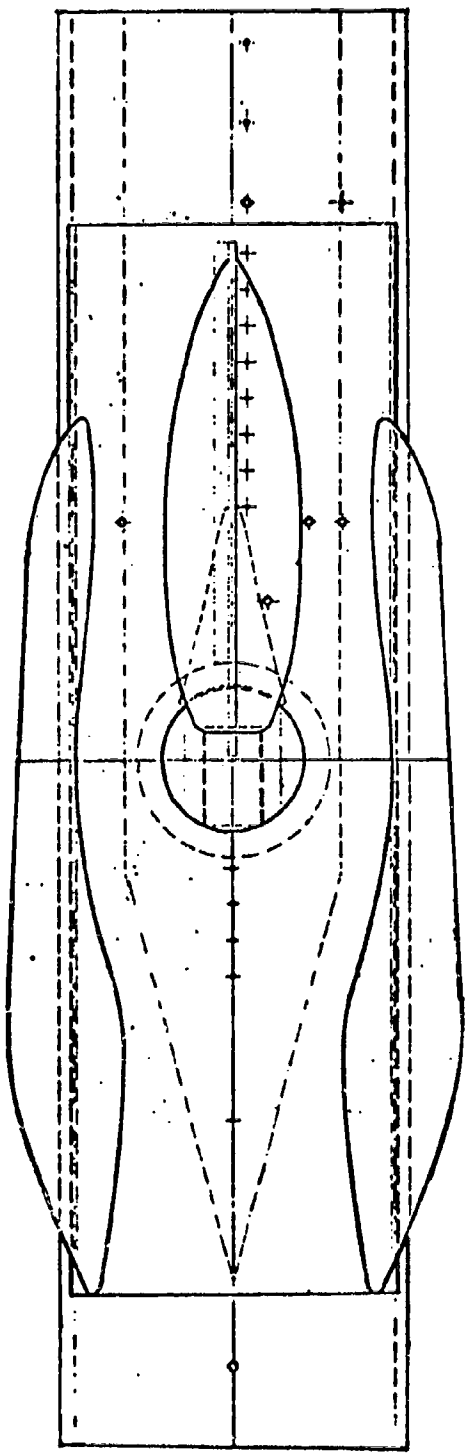

Fig. 34. Top View of Model 4

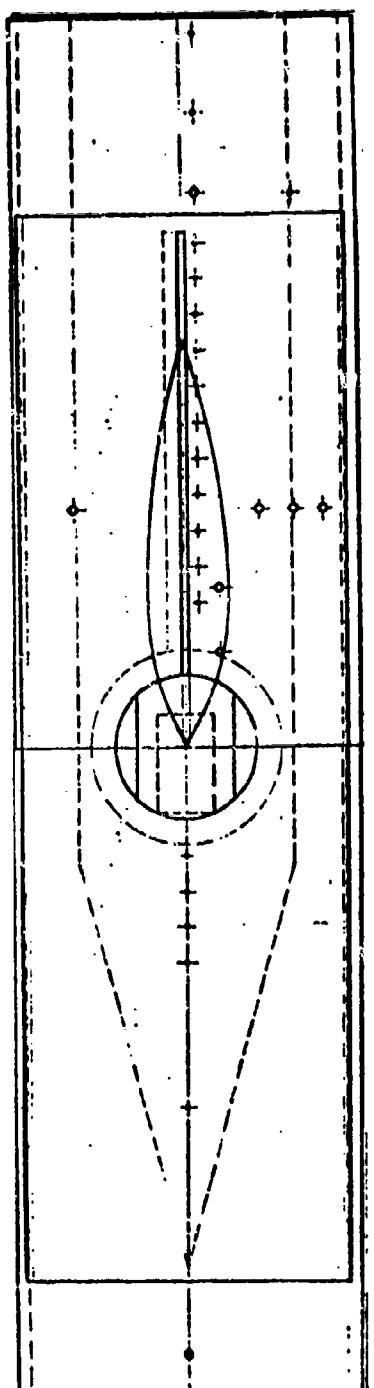

Fig. 35. Top View of Model 6

Appendix B

Drag versus Mach Number

This Appendix contains values of Drag coefficient for all configurations. Each model was tested at an azimuth angle of 0^{o} and 90^{o} and a constant Reynolds number of $4x10^{5}$ unless otherwise noted. The reference area used in computing the drag coefficient was the turret frontal area, S_t, 0.047 ft^2.

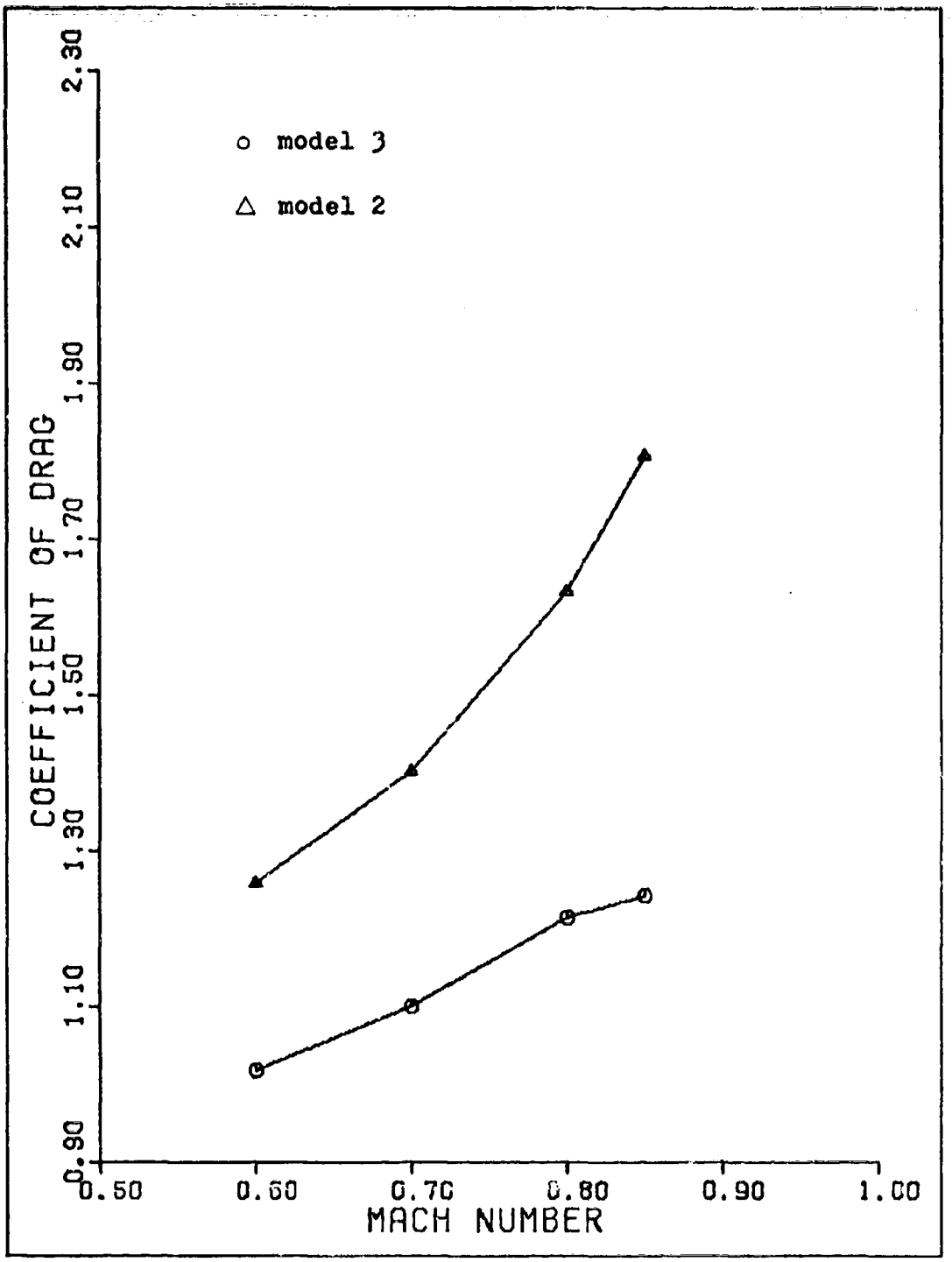

Fig. 36. Drag Coefficients for Models 2 and 3, $\Delta 1\text{-}0^{\circ}$

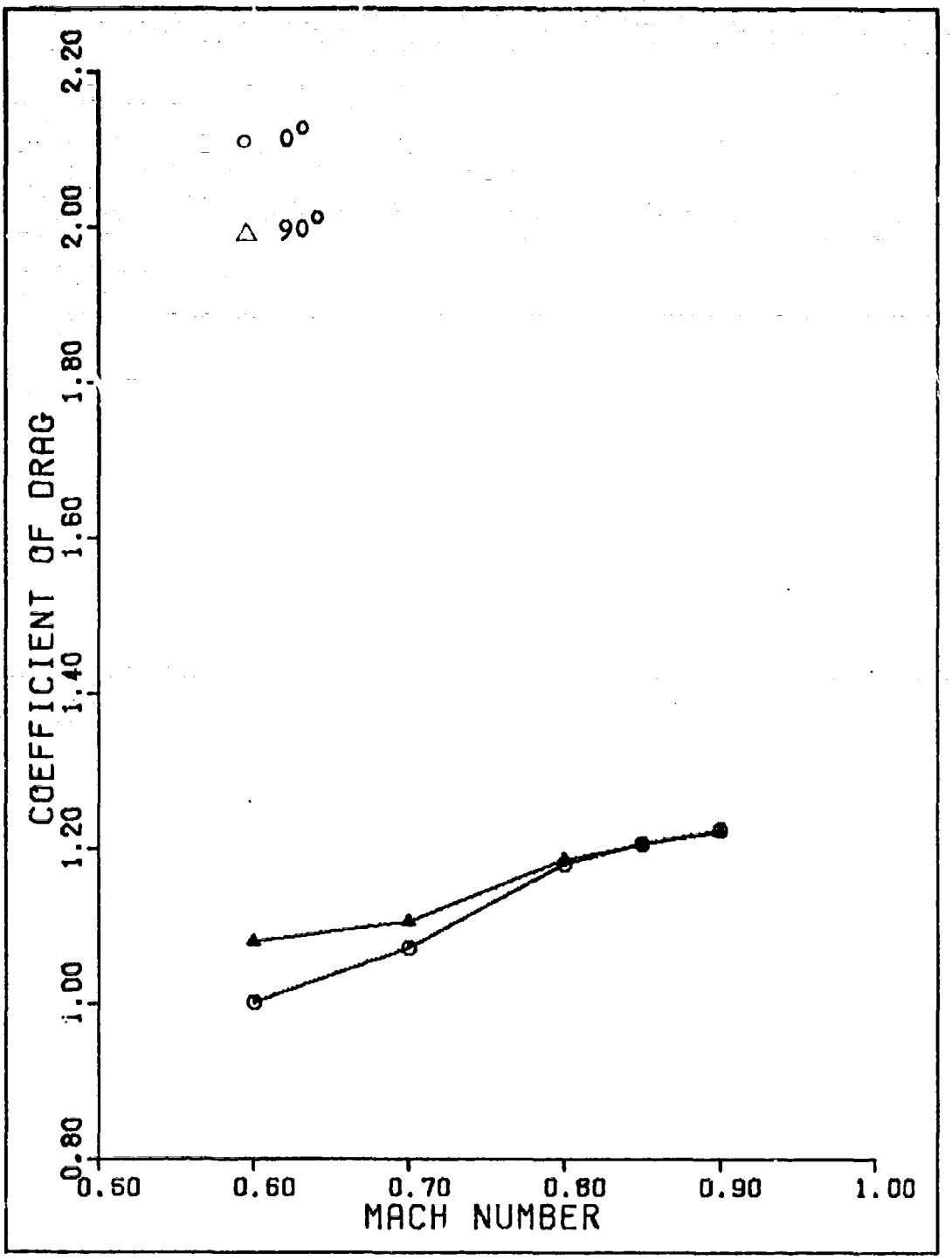

Fig. 37. Drag Coefficients for Model 4

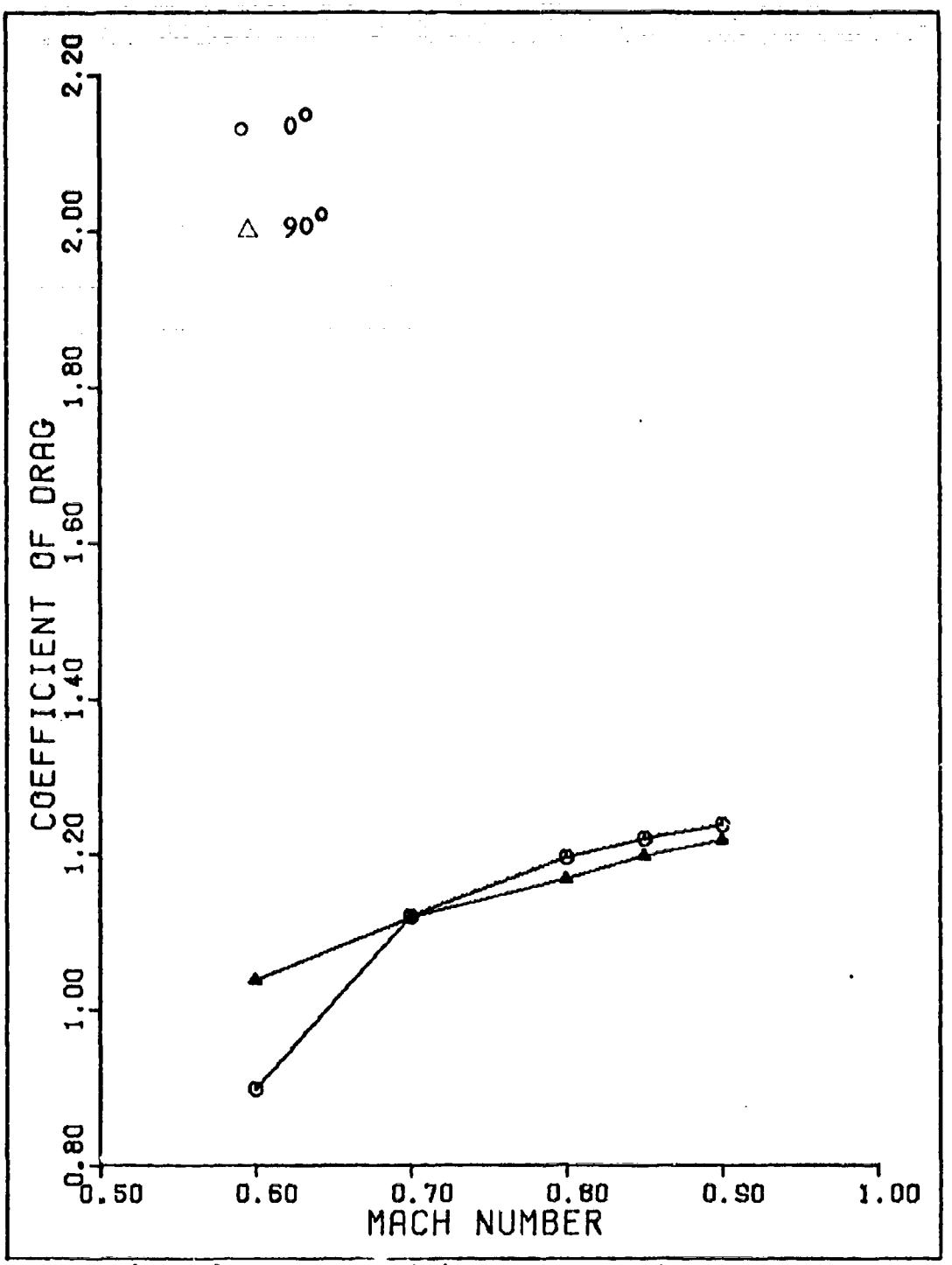

Fig. 38 Drag Coefficients for Model 5

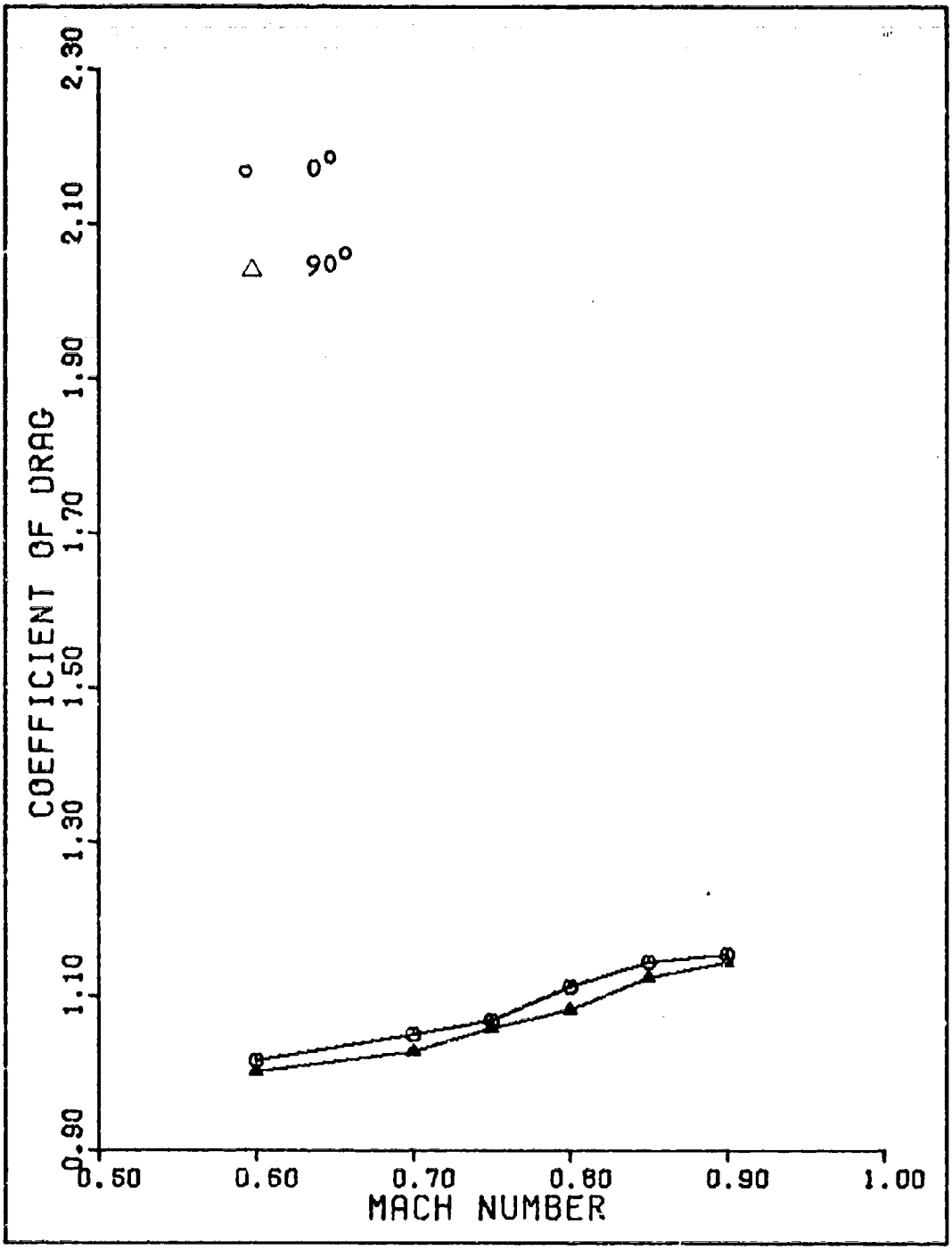

Fig. 39. Drag Coefficients for Model 6

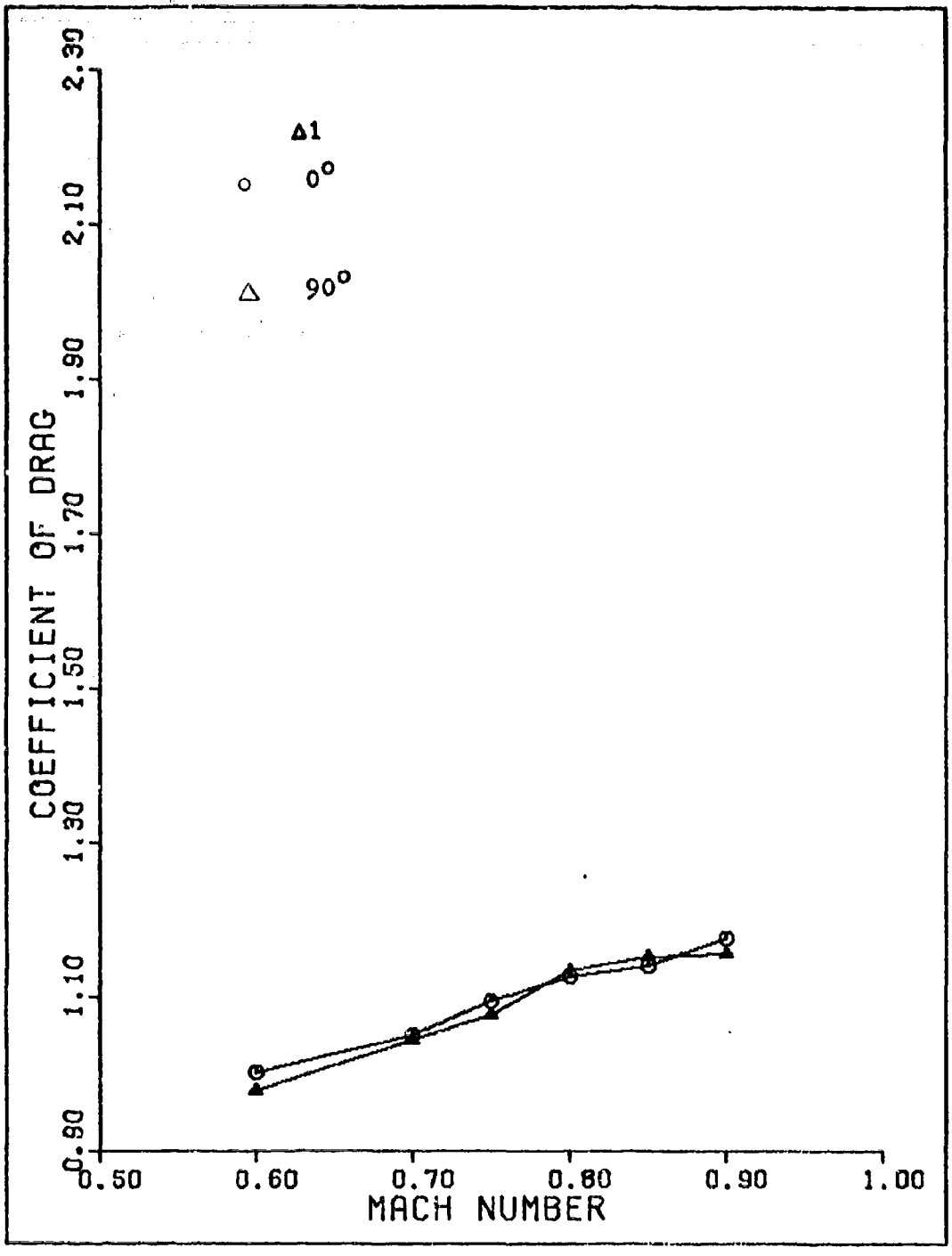

Fig. 40. Drag Coefficients for Model 7

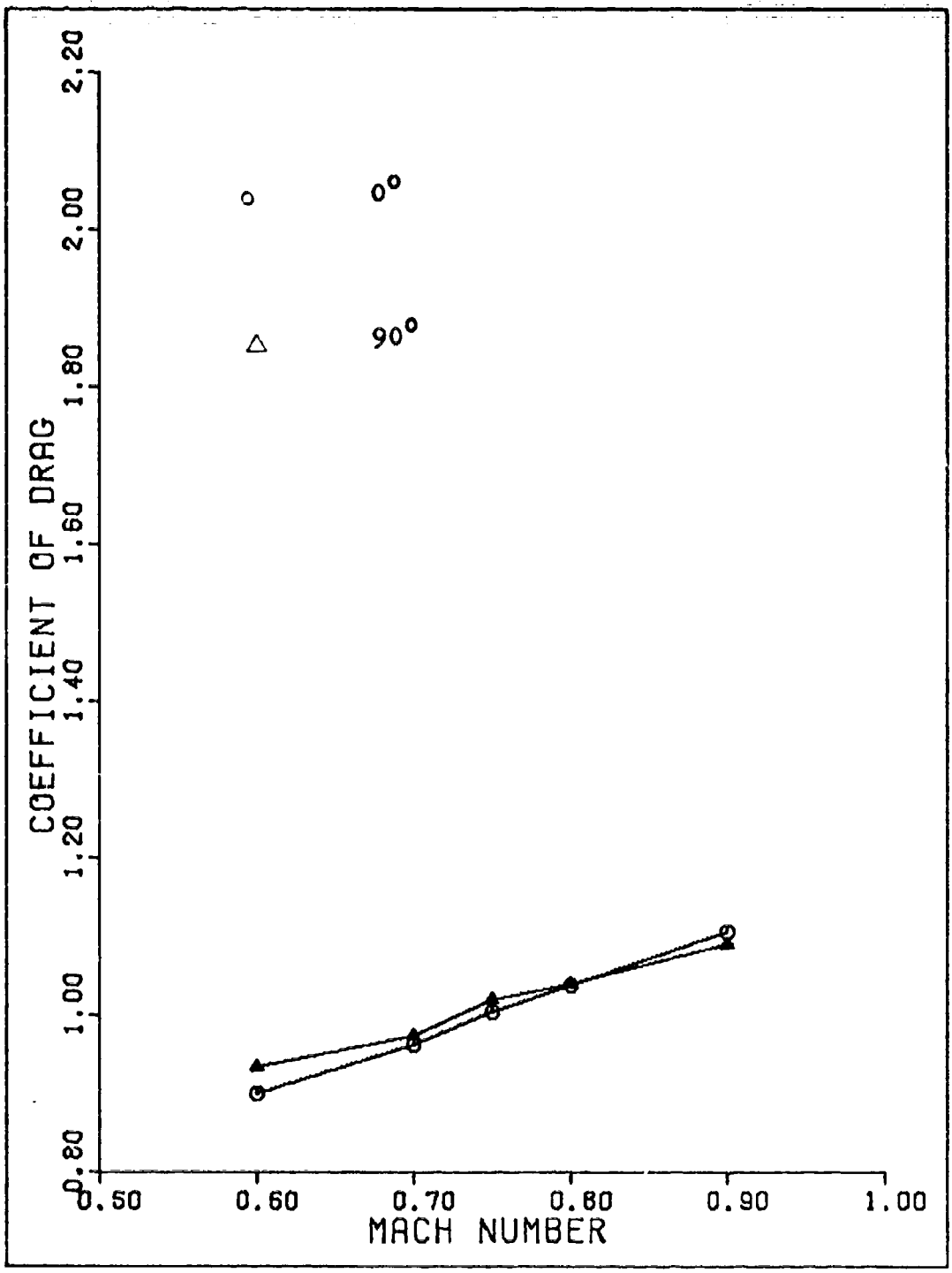

Fig. 41. Drag Coefficients for Model 8

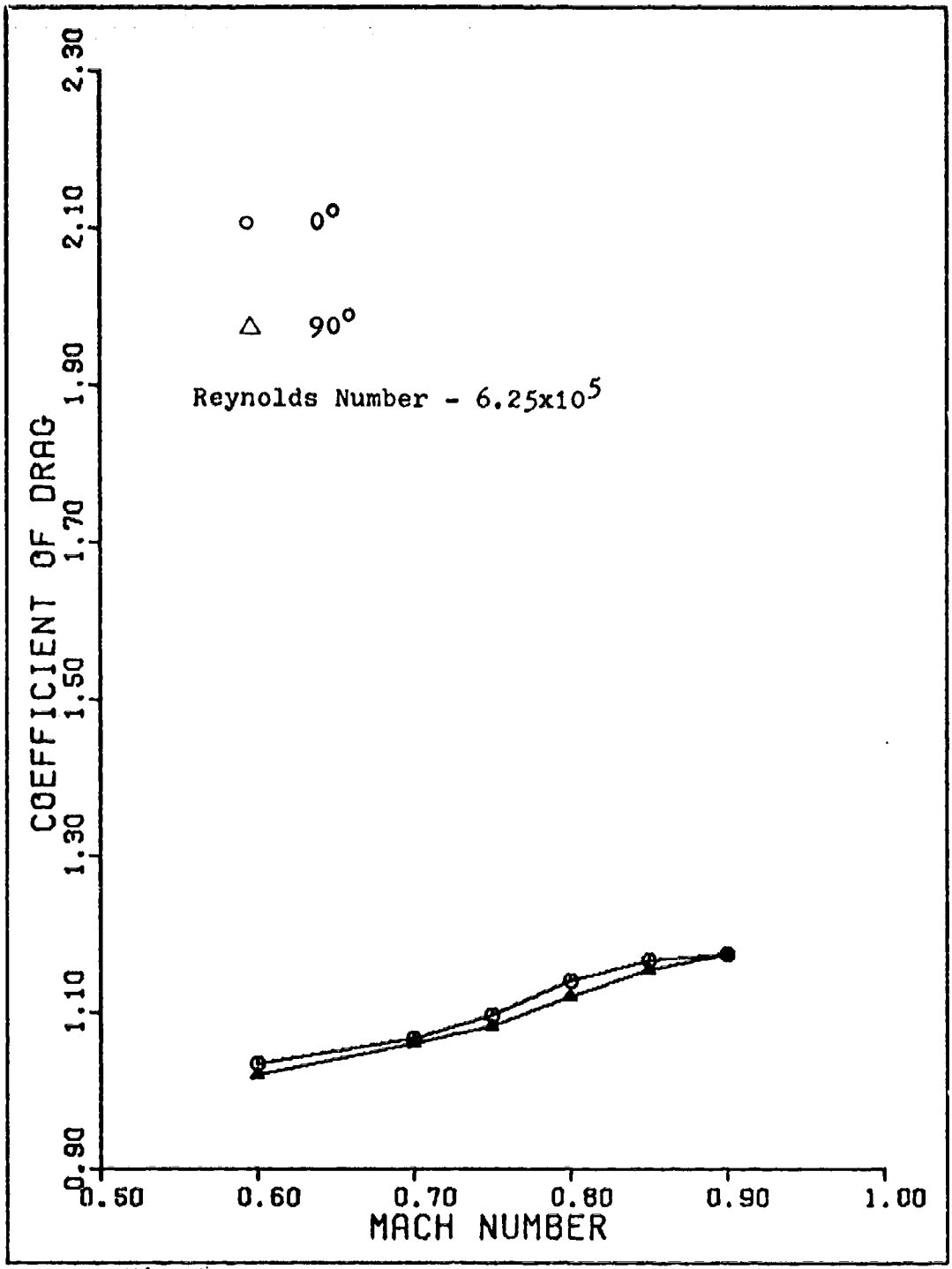

Fig. 42. Drag Coefficients for Model 6

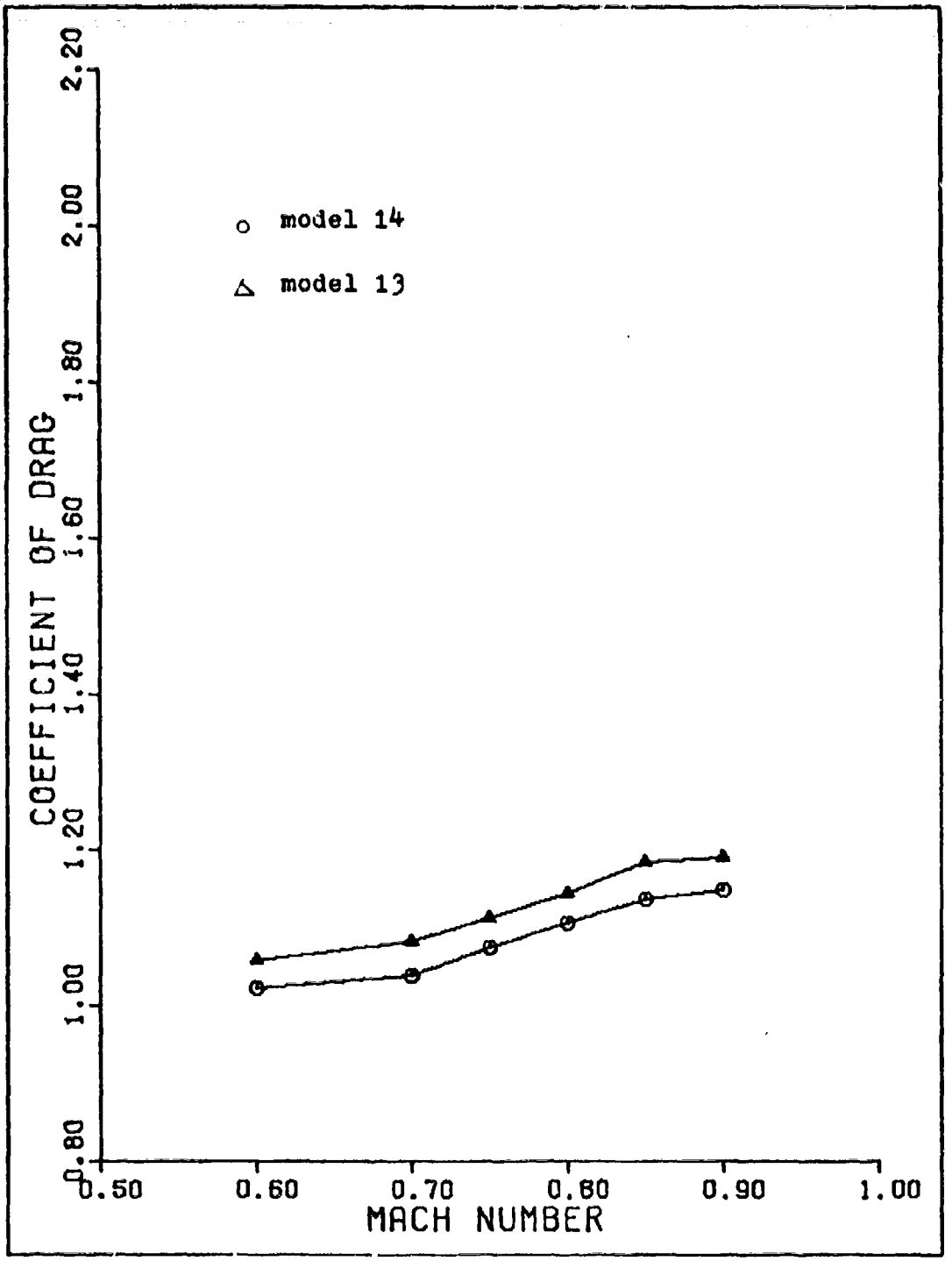

Fig. 43. Drag Coefficients for Models 6 and 7 Without Force Balance Bridged

Appendix C

Oil Flow Visualization Drawings

This Appendix contains Figures 88 thru 90 which are the oil flow patterns that were observed on the models. Only model 7 is included because the interesting pattern formed on its side fairings was the only one of significance.

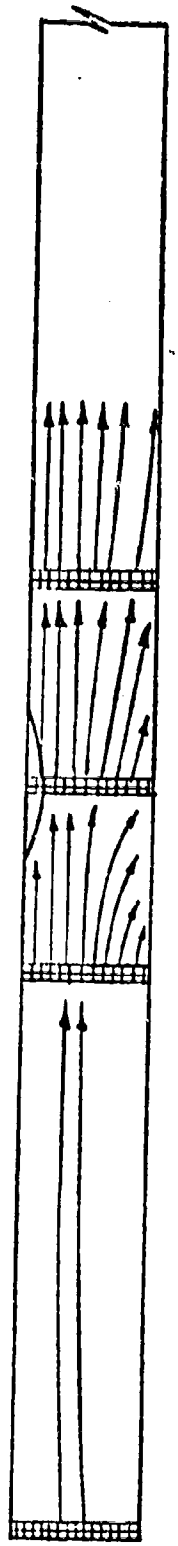

Fig. 44. Oil Flow on Configuration 1 for Mach 0.6

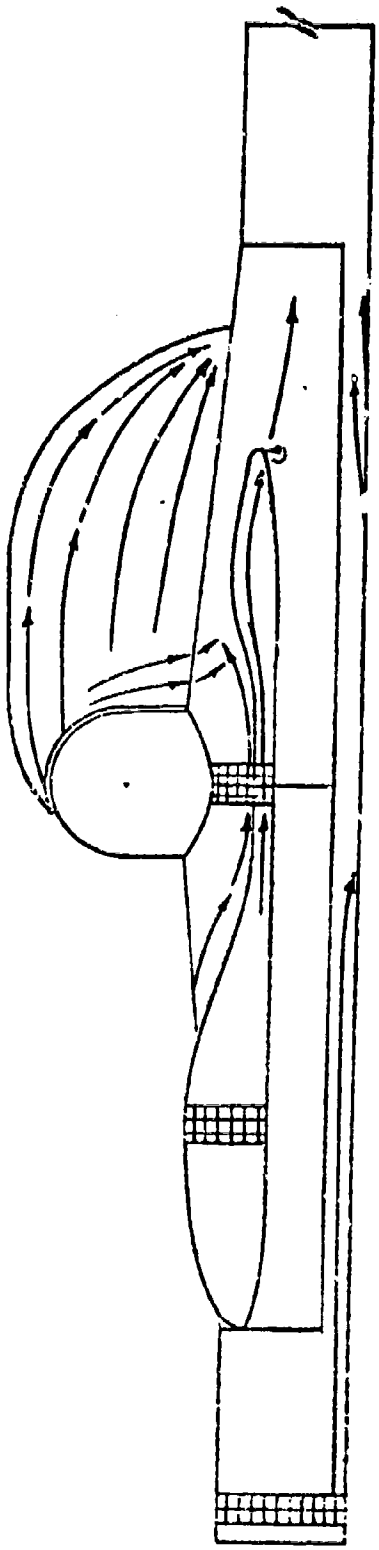

Fig. 45. Oil Flow on Configuration 7

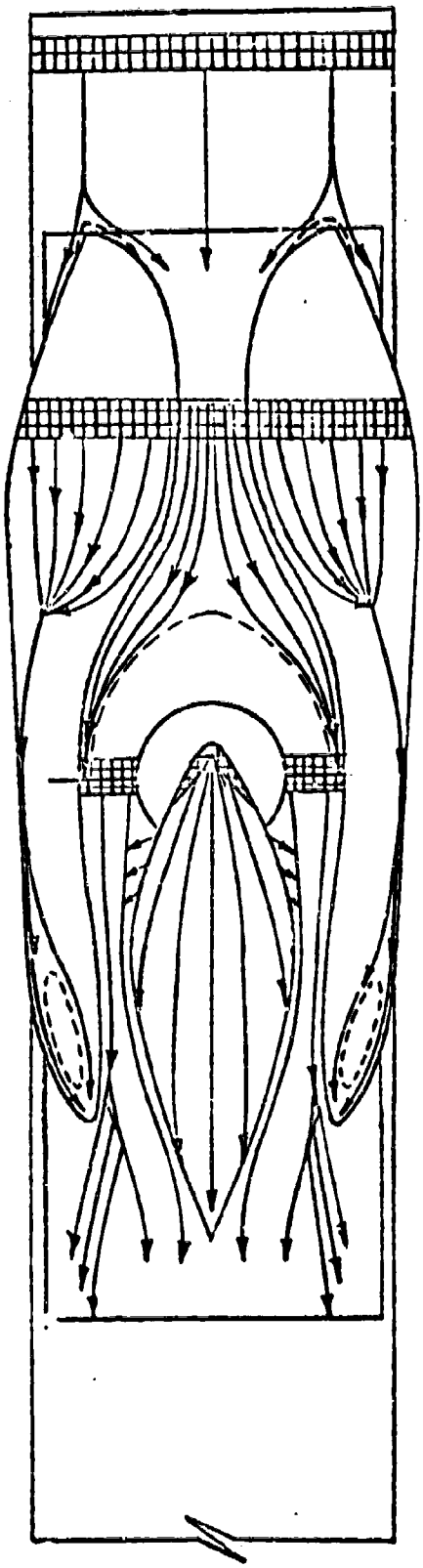

Fig. 46. Oil Flow on Configuration 7

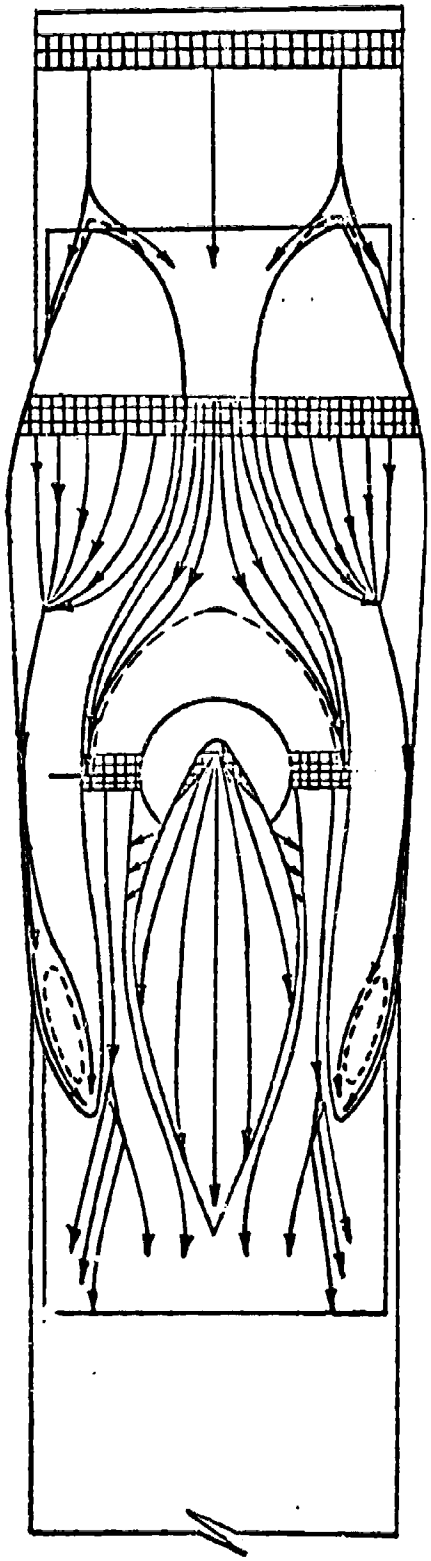

Fig. 46. Oil Flow on Configuration 7

Vita

Steve B. Borah was born in St. Louis, Missouri on 31 January 1946. Graduating in 1964 from Whetstone High School, Columbus, Ohio, he then attended the United States Air Force Academy where he received the degree of Bachelor of Science in Engineering Sciences in 1968. After the completion of flying training in 1969, he was assigned to Southeast Asia as a forward air controller. In 1971, he was transfered to Beale AFB, as a KC-135 pilot where he remained until his entrance into the Air Force Institute of Technology.

Permanent Address: 4843 Bourke Rd.
Columbus, Ohio
43229

This thesis was typed by Mrs. Cynthia W. Borah